

Long ties accelerate noisy threshold-based contagions

Dean Eckles^{a,b,2}, Elchanan Mossel^{a,c,2}, M. Amin Rahimian^{a,2}, and Subhabrata Sen^{c,2}

^aInstitute for Data, Systems, and Society; ^bSloan School of Management; ^cDepartment of Mathematics ,
Massachusetts Institute of Technology, Cambridge, MA 02139

Working paper. November 22, 2023.

Changes to network structure can substantially affect when and how widely new ideas, products, and conventions are adopted. In models of biological contagion, interventions that randomly rewire edges (generally making them “longer”) accelerate spread. However, there are other models relevant to social contagion, such as those motivated by myopic best-response in games with strategic complements, in which individual’s behavior is described by a threshold number of adopting neighbors above which adoption occurs (i.e., complex contagions). Recent work has argued that highly clustered, rather than random, networks facilitate spread of these complex contagions. This conclusion is based primarily on theoretical and simulation results assuming adoption never occurs with only one adopting neighbor. Here we show that minor modifications to this model, which make it more realistic, reverse this result. The modification is that we allow very rarely below threshold adoption, i.e., very rarely adoption occurs, where there is only one adopting neighbor. To model the trade-off between long and short edges we consider networks that are the union of cycle-power- k graphs and random graphs on n nodes. We study how the time to global spread changes as we replace the cycle edges with (random) long ties. Allowing adoptions below threshold to occur with order $1/\sqrt{n}$ probability is enough to ensure that random rewiring accelerates spread. Simulations illustrate the robustness of these results to other commonly-posed models for noisy best-response behavior. We then examine empirical social networks, where we find that hypothetical interventions that (a) randomly rewire existing edges or (b) add random edges reduce time to spread compared with the original network or addition of “short”, triad-closing edges, respectively. This substantially revises conclusions about how interventions change the spread of behavior, suggesting that those wanting to increase spread should induce formation of long ties, rather than triad-closing ties. More generally, this highlights the importance of noise in game-theoretic analyses of behavior.

Keywords: social networks | game dynamics | social contagion

Authors are listed in alphabetical order. D.E., E.M., M.A.R., and S.S. designed research, performed research, contributed new analytic tools, analyzed data, and wrote the paper.

D.E. has a significant financial interest in Facebook. E.M., M.A.R. and S.S. declare no conflict of interest.

²To whom correspondence should be addressed: {eckles,elmos,rahimian,ssen90}@mit.edu

Social interactions among individuals facilitate a diverse range of contagions, including both biological contagions and the spread of ideas, products, and conventions (i.e., social contagion). Empirical research supports the conclusion that social contagion is ubiquitous, finding it in many behaviors, such as product adoption (1–9), political participation (10–12), exercise (13), and (mis)information (14, 15). Other work presents evidence of contagion between political entities (16, 17) and non-human animals (18–21). Indeed, social contagion is central to all social and behavioral sciences, and knowledge of contagion has implications for many applied sciences. For example, decision-makers may rely on a model of contagion in planning interventions that seed a behavior (3, 22–25), prevent or reverse infection of nodes (26–28), or that attempt to modify network structure (29–32).

Social contagion is often described and modeled by analogy to biological contagion of infectious disease. Such *simple contagion* models typically posit that there is no interdependency between multiple network neighbors: a vertex has an independent (and typically identical) probability of being infected by each infected neighbor (33). This corresponds to the sublinear activation functions, which specify the probability of adoption as a function of the number of adopters in the network neighborhood, shown in Figure 1A. Such contagions spread more slowly in highly clustered networks than in more random networks (34, 35). Addition of random (“long”) ties to a highly-clustered network allows a contagion to rapidly spread to other areas of the network. For social contagions that are expected to be driven by transfer of information, such a model, in which each neighbor with the information has some probability of transmitting it, is theoretically appealing. Related considerations lead to the “strength of weak ties” hypothesis by which “weak” (or more properly “long”) ties play critical roles in access to information (36), such as in labor markets (cf. 37).

If, instead of a transfer of a pathogen or simple information, adoption requires receiving more complex information or it occurs because of normative social pressure or attempts to coordinate, such a model may seem inadequate (38, 39). Threshold models are the archetypal activation functions for a *complex contagion* (40, 41). They can be rationalized as myopic best-response dynamics in a sequence of repeated semi-anonymous graphical games (42) with strategic complements (such as in coordination games), whereby vertices’ utilities from adopting depend on the number of adopting neighbors (43–45). If vertices share a homogeneous utility function, then such a model has a single parameter θ that specifies a threshold activation function dividing non-adoption from adoption (Figure 1B); call this *deterministic θ -complex contagion*.

Clearly complex contagions can be differently affected by network structure than simple contagions. An extreme case is straightforward: consider the spread of deterministic, 2-complex contagion on the 2-regular circular lattice structure shown in the middle Figure 2. Infecting any two adjacent nodes on the circle will cause the entire graph to be infected after four time steps. However, rewiring any of the edges that is not connecting the initial infected nodes (“seeds”) and replacing it with a long tie across the circle prevents the global spread of the deterministic, 2-complex contagion. Thus, interventions that rewire edges randomly may prevent total spread, and interventions that add random edges may be less effective at facilitating spread than interventions that add triad-closing edges. Along these lines, recent work has argued that the spread of complex contagions, unlike simple contagions, is facilitated by more clustered networks (41, 46–48).

Is such a deterministic model realistic? Empirical studies of social contagion, including those

that ostensibly provide evidence for complex contagion, find substantial probability of adoption with a single adopting neighbor (22, 49–51). Rather than positing determinism, analyses of discrete choice problems typically hypothesize that individuals are random utility maximizers. Specific noise distributions then rationalize choice probabilities specified, e.g., probit and logit functions. In a probit activation function the probability of adoption with x adopters in the social neighborhood is equal to $\Phi_{\theta,\sigma}(x)$, where $\Phi_{\theta,\sigma}(\cdot)$ is the normal CDF with mean θ and standard deviation σ . The logit activation function is given by $\Psi_{\theta,\sigma}(x) = (1 + e^{(\theta-x)/\sigma})^{-1}$. Both functions describe a noisy threshold response that converges to a deterministic threshold θ as $\sigma \rightarrow 0$. Some of the recent ideas surrounding the “weakness of long ties” that argue the spread of complex contagions is facilitated by more clustered networks (41, 46) are motivated by deterministic thresholds or limits as $\sigma \rightarrow 0$. As such, these results are less informative about realistic versions of complex contagions in which adoptions occur below the threshold. Here we show that introducing a small probability of below-threshold adoption (denoted by q in Figure 1B), even only via some short ties, reverses existing stylized facts about how network structure affects the spread of complex contagions. This somewhat harmonizes theoretical guidance about how network structure affects the spread of both simple and complex contagions.

Comparison to Related Work

Our results fall in the general category of work that addresses how network structure affects social contagions (4, 45, 46). This question has been studied by researchers in many fields, including applied probability (52, 53), computer science (54–57), physics (47), economics (58), and sociology (41). We analyze these effects in the canonical case of 2-complex contagions. In a d -regular graph this corresponds to the linear threshold model (23, 40) with fixed (relative) thresholds set to $2/d$. Using an absolute threshold allows us to isolate the effect of structural interventions irrespective of the initial seed sets.* Our characterization is in terms of time to global spread. Our results are in the same spirit as the studies of the linear threshold model that relate the extent of spread to structural properties of networks, and in particular, “cohesiveness” (44, 59), suggesting that innovations spread further across networks that are less cohesive. In contrast, *we analyze the time to spread in realistic 2-complex contagions (allowing for adoptions below threshold with probability q) and show that innovations spread faster in less clustered networks.*

Janson et al. (52) study the threshold spreading process (referred to as bootstrap percolation in the applied probability literature) using a mean-field approximation. They use a random graph model that is the union of lattice with random (long) edges. The lattice structure provides for local clustering, while the random (long) ties decrease the network diameter. Both these features (high clustering and a small diameter) are observed in real network data and are the basis for the Watts–Strogatz small-world random graph model (60), where the edges of a cycle-power- k (\mathcal{C}_k)[†] graph are rewired and replaced by random long ties. The

*For example, introduction of a new edge has a monotone increasing influence on the spreading rate in an absolute threshold model; whereas, if thresholds are specified with respect to the ratio of adopters in each neighborhood, then depending on the size and location of adopters one can place the new edges carefully to impede the spread.

[†]The cycle-power- k graph, denoted by \mathcal{C}_k , is constructed by connecting each node on an n -cycle to all nodes within its k -hop distance (i.e. the $2k$ nearest neighbors), where the hop distance is measured on the cycle \mathcal{C}_1 .

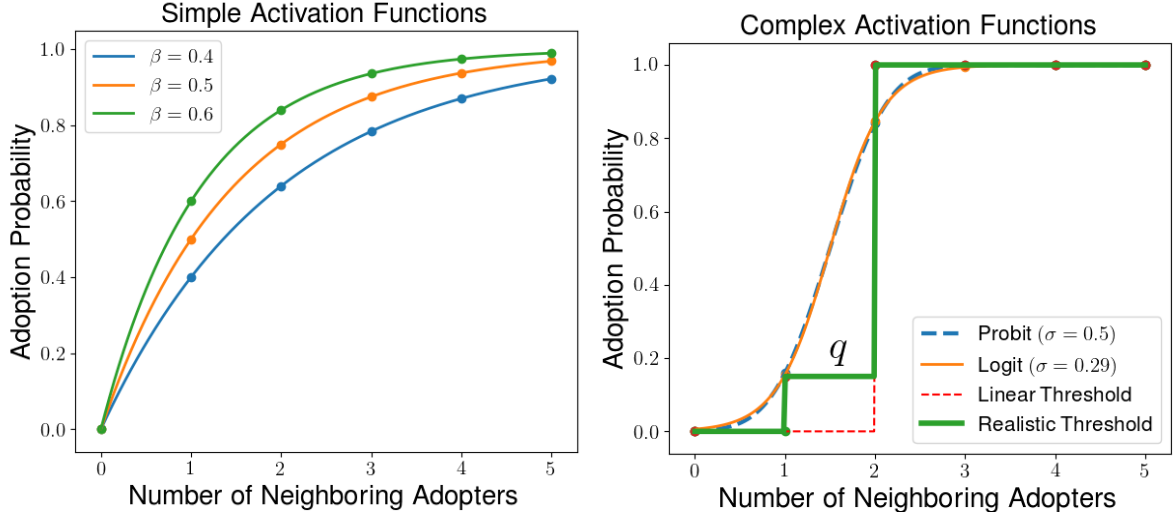


Fig. 1. Activation functions for (A) simple contagion and (B) variations on complex contagion. In the case of a simple activation function (A), every edge has an independent probability β of transmitting infections (adoptions); subsequently, the probability of adoption with x adopters in the social neighborhood is given by $1 - (1 - \beta)^x$. In the case of a realistic threshold-based contagion model (B), there is a non-zero probability ($q > 0$) of adoptions below threshold.

Watts–Strogatz model is suitable for studying the effect of network structure and interventions that modify local clustering. For the most part, we consider the more analytically amenable Newman–Watts model (61) in which random edges are added on top of \mathcal{C}_k . The spread of threshold processes have been also analyzed in a variety of other random graph models, including random regular graphs, power-law and configuration models (54–57, 62–64).

We are interested in realistic models of complex contagion which allow for adoptions below threshold. Focusing on the canonical case of 2-complex contagion, we allow for a probability of (simple) adoptions with a single neighboring adopter and denote this probability by q_n , where n is the network size. We show that having[‡] $q_n = \omega(1/\sqrt{n})$ is enough to change the landscape of results leading to weakness of long ties for complex contagions. Our following results indicate that *long ties accelerate realistic complex contagions*.

Results

Consider the cycle-power- k graph (\mathcal{C}_k). Starting from a pair of adjacent (\mathcal{C}_1 -neighboring) infected nodes, it takes n/k time steps for all the n nodes on \mathcal{C}_k to get infected via pure 2-complex contagion. We examine the spreading speed of contagion as the cycle edges (short ties) are removed and replaced with random edges (long/weak ties). To this end, we first analyze the spread of contagion on the union graph $\mathcal{C}_k \cup \mathcal{G}_{n,p_n}$, where \mathcal{G}_{n,p_n} is the Erdős–Rényi

[‡]Given three functions $f(\cdot)$, $g(\cdot)$, and $h(\cdot)$ we use the asymptotic notations $f(n) = O(g(n))$ and $f(n) = o(h(n))$ to signify the relations $\limsup_{n \rightarrow \infty} |f(n)/g(n)| < \infty$ and $\lim_{n \rightarrow \infty} |f(n)/h(n)| = 0$, respectively; in the latter case we also write $h(n) = \omega(f(n))$. We use $f(n) = \Omega(g(n))$ to signify $\liminf_{n \rightarrow \infty} f(n)/g(n) > 0$. We use $f(n) = \Theta(g(n))$ to mean that $f(n) = O(g(n))$ and $f(n) = \Omega(g(n))$. We sometimes describe the asymptotic orders up to a logarithmic factor and use $O^*(f(n))$ to mean $O(f(n) \log^\alpha(n))$ for some fixed α .

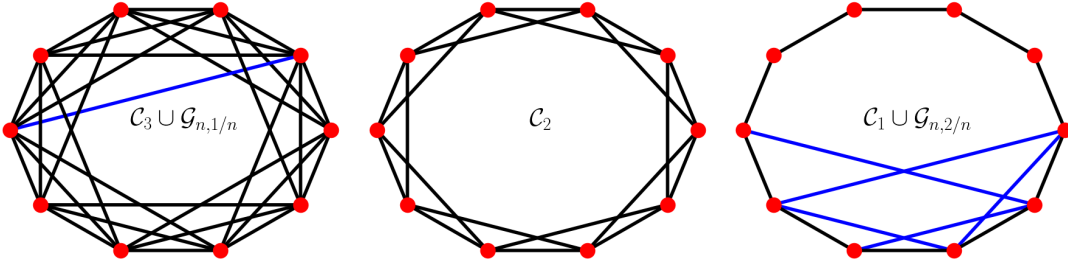


Fig. 2. Unions of cycle-graphs and random graphs. The cycle edges are colored black and random (long) edges are colored blue.

random graph model with edge probability p_n . We note that the union graph has n vertices and set of edges is the union of edges in the two graphs. Setting $p_n = (D - 2k)/n$ ensures that the expected degree of each node is kept fixed at D . Thus by varying k , we can study the spreading rate of contagion as the cycle edges are rewired and replaced by (random) long ties.

Theorem 1 derives the asymptotic rate of spread for 2-complex contagion on $\mathcal{C}_2 \cup \mathcal{G}_{n,c/n}$. Our result immediately implies that the rate is faster than pure 2-complex contagion on $\mathcal{C}_{2+c/2}$, thus emphasizing the usefulness of long ties in speeding up complex contagion as long as the required local structure (the cycle \mathcal{C}_2) is intact.

Theorems 2 and 3 study the rate of spread of complex contagion as the edges of \mathcal{C}_2 are rewired; this alters the short tie structure that is necessary for the local diffusion of complex contagion. To facilitate the spread of complex contagion to the entire graph, we allow for a small probability q_n of *adoptions below threshold*. Formally, this implies that a vertex with at least one infected neighbor gets infected independently in each round with probability q_n . We rewire the $\mathcal{C}_2 \setminus \mathcal{C}_1$ edges, keeping the average degree constant (equal to four). We interpolate between \mathcal{C}_2 and $\mathcal{C}_1 \cup \mathcal{G}_{n,2/n}$ by rewiring the edges on $\mathcal{C}_2 \setminus \mathcal{C}_1$. Theorem 2 establishes that if the probability of sub-threshold adoptions is large enough ($\sqrt{n}q_n \rightarrow \infty$), the contagion spreads faster in $\mathcal{C}_1 \cup \mathcal{G}_{n,2/n}$, compared to \mathcal{C}_2 . Theorem 3 provides a more detailed picture, and analyzes the spreading time at any point on the interpolation path between \mathcal{C}_2 and $\mathcal{C}_1 \cup \mathcal{G}_{n,2/n}$. At first, as we rewire $o(\sqrt{n})$ edges, the time to spread increases. In this scenario, there are too few long ties to facilitate complex contagion to faraway nodes. On the other hand, the missing double edges incur a waiting time, thus slowing down the total time required. However, once $\omega(\sqrt{n})$ edges have been rewired, complex contagion spreads along the long ties. If $\sqrt{n}q_n \rightarrow \infty$, complex contagion via long ties facilitates the spread of contagion to the whole graph in $o(n)$ time. Note that this is much faster than the original spreading time over \mathcal{C}_2 .

Before stating our results formally, we identify some of the mechanisms that govern the spreading rate of the contagion over $\mathcal{C}_k \cup \mathcal{G}_{n,p_n}$ graphs. The contagion is initialized by two infected neighbors on \mathcal{C}_1 . The contagion spreads through two distinct sub-processes: (i) spreading along the cycle \mathcal{C}_1 via simple and complex contagion, and (ii) complex contagion along the long (“weak”) ties. The latter occurs when an uninfected node has at least two long ties connecting it to infected vertices. Initially, the infection spreads along the cycle. Once the infected nodes form intervals of sufficient length, the infection can spread to far away parts of the graph using the long ties. All our results hold with high probability (w.h.p.), i.e., with

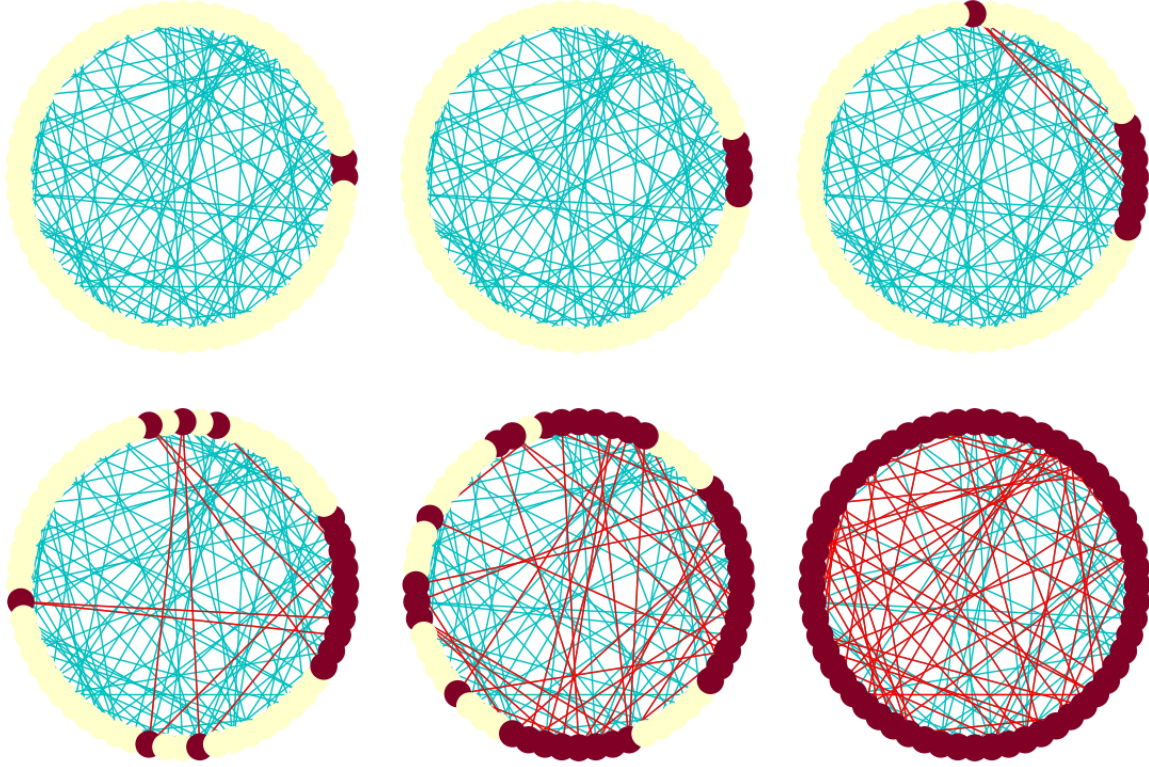


Fig. 3. Illustration of spreading via short and long ties. Each node is connected to its four nearest neighbors on the cycle (\mathcal{C}_2) and, in addition, has two (random) long ties. The contagion spreads locally via the short ties of \mathcal{C}_2 . Then there are multiple ties from the infected interval to the distant vertices, resulting in the contagion jumping across the cycle. The red links in the figure are between the existing and newly infected nodes. They highlight the “path” of the spread. When two (red) links from an infected interval land on the same “faraway” node, they form a “wide” enough bridge for the complex contagion to cross.

probability converging to one as the number of nodes $n \rightarrow \infty$.

Speed of Complex Contagion with Long Ties. In this section, we provide the asymptotic rate of 2-complex contagion over $\mathcal{C}_2 \cup \mathcal{G}_{n,c/n}$, and compare it with the spread over $\mathcal{C}_{2+c/2}$. Complex contagion in the latter case, takes $n/(2 + c/2) = \Theta(n)$ time steps to spread. Our analysis below establishes that the diffusion time in $\mathcal{C}_2 \cup \mathcal{G}_{n,c/n}$ is $O^*(n^{3/4})$, significantly faster than $\Theta(n)$. In fact, we show that the spreading time is w.h.p. greater than $o(n^{3/4})$, thus essentially fixing the order of the spreading time at $n^{3/4}$ (up to some logarithmic factors).

Our result emphasizes the intuitive understanding that rewiring accelerates the spread of complex contagion (from $\Theta(n)$ in $\mathcal{C}_{2+c/2}$ to $O^*(n^{3/4})$ in $\mathcal{C}_2 \cup \mathcal{G}_{n,c/n}$), as long as the essential short tie structure (in our case \mathcal{C}_2) that facilitates local reinforcements, remains intact.

Theorem 1 (Rate of 2-complex contagion over $\mathcal{C}_2 \cup \mathcal{G}_{n,c/n}$). *The time to total spread in $\mathcal{C}_2 \cup \mathcal{G}_{n,c/n}$ can be upper and lower bounded as follows:*

- (i) *The entire graph is infected in time $2n^{3/4}(\log \log n)^2$, w.h.p.*
- (ii) *For any $\varepsilon > 0$, the number of nodes infected by time $n^{3/4-\varepsilon}$ is at most \sqrt{n} w.h.p.*

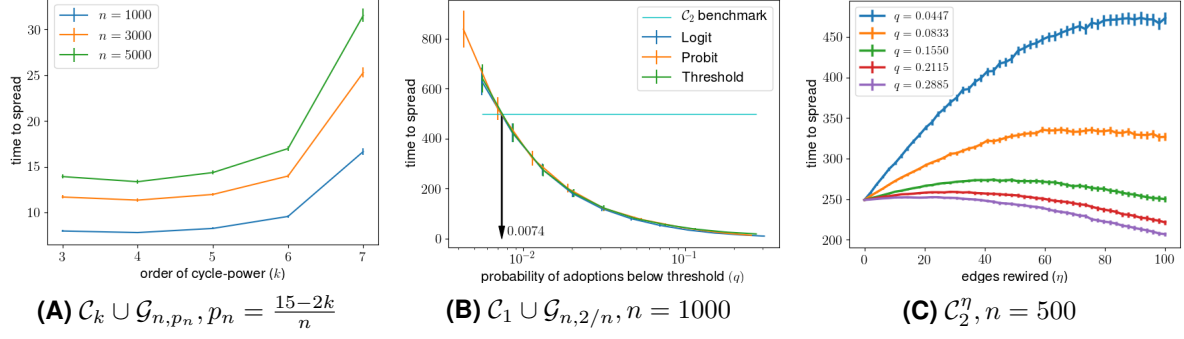


Fig. 4. Spreading time of complex contagion over cycle-power union random graphs with a fixed overall expected degree D , (A) $D = 15$, (B) $D = 4$ and (C) $D = 4$. The spreading model in (A) is the 2-complex contagion (with no simple/sub-threshold adoptions, as in Theorem 1). In (B), again, we consider 2-complex contagion but allow a simple adoption probability q on every edge. In (C), we follow the same model as in Theorem 3: 2-complex contagion with sub-threshold adoption probability q only along the \mathcal{C}_1 cycle edges. Each point is the average of 100, 500, and 1000 random draws for (A), (B), and (C), respectively. The vertical bars indicate the 95% normal confidence intervals around the means.

In (54) the authors bound the spreading time of 2-complex contagion in the related Newman-Watts random graph model (65) by $\Omega(\sqrt{n/\log n})$ and $O(\sqrt[5]{n^4 \log n})$. Our results suggest that the order of the spreading time can be characterized more precisely as $O^*(n^{3/4})$.

Figure 4 shows the time that it takes for the contagion to spread over $\mathcal{C}_k \cup \mathcal{G}_{n,(D-2k)/n}$ graphs. The expected degree is fixed at D , which is set to $D = 15$ in Figure 4A. Simulation results show that rewiring the cycle edges and replacing them with random long ties speeds up the spread of contagion. However, this trend is not carried through all the way until $k = 2$. Note that if we rewire the cycle edges beyond \mathcal{C}_2 , complex contagion may not spread to the entire graph. However, allowing a vanishing probability ($q \rightarrow 0$) of simple adoptions along the cycle edges will circumvent this issue. Our subsequent results in Theorems 2 and 3 address this case.

Speed of Complex Contagion with Simple Adoptions. We introduce and study a model where in addition to complex contagion we have a small amount of simple contagion along the \mathcal{C}_1 edges, i.e. contagion can spread with (small) probability $q := q_n$ along \mathcal{C}_1 . We will suppress the dependence of q on n whenever clear from the context. In this setup, we compare the diffusion speed between $\mathcal{C}_1 \cup \mathcal{G}_{n,2/n}$ and \mathcal{C}_2 . We conclude that for large enough q (having $\sqrt{n}q \rightarrow \infty$ turns out to be enough), contagion spreads faster in $\mathcal{C}_1 \cup \mathcal{G}_{n,2/n}$ compared to \mathcal{C}_2 . Hence, rewiring all the \mathcal{C}_2 edges but keeping the \mathcal{C}_1 edges intact, will speed up the spread of complex contagions, provided that there is a high enough (but vanishing with increasing n) probability of simple adoptions along the cycle-edges. The next theorem establishes that the rate of 2-complex contagion (with q simple adoptions) over $\mathcal{C}_1 \cup \mathcal{G}_{n,2/n}$ is of order \sqrt{n}/q . Formally, we establish the following result.

Theorem 2 (Rate of 2-complex contagion over $\mathcal{C}_1 \cup \mathcal{G}_{n,2/n}$ with simple adoptions probability q). *Allowing for simple adoptions to occur with probability q along \mathcal{C}_1 , the time to total spread*

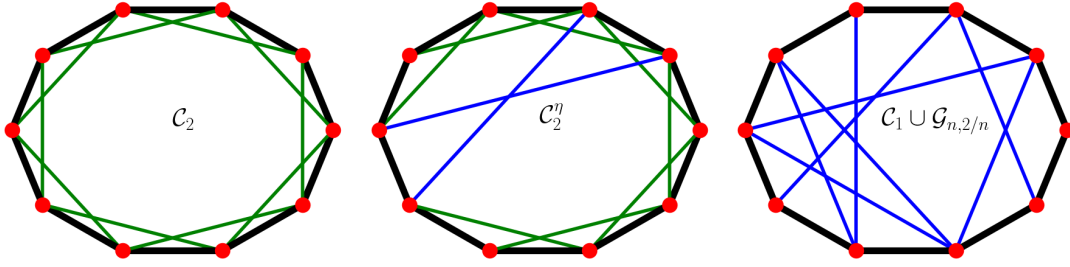


Fig. 5. In Theorems 2 and 3, we characterize the speed of spread as $\mathcal{C}_2 \setminus \mathcal{C}_1$ edges (in green) are removed and replaced by random long ties (in blue), allowing for simple contagions only along the edges of \mathcal{C}_1 (in black).

in $\mathcal{C}_1 \cup \mathcal{G}_{n,2/n}$ can be upper and lower bounded as follows:

- (i) The entire graph is infected by time $\frac{4\sqrt{n}}{q}(\log \log n)^2$ w.h.p.
- (ii) For any $\varepsilon > 0$, up to time $n^{1/2-\varepsilon}/q$, the number of infected nodes is at most \sqrt{n} w.h.p.

Figure 4B shows the spreading rate of contagion over $\mathcal{C}_1 \cup \mathcal{G}_{n,2/n}$ with $n = 1000$. We use three activation functions: logit, probit, and modified threshold with non-zero probability (q) of adoptions below threshold. Indeed, logit and probit functions even allow for spontaneous adoptions (when there are no infected neighbors). Moreover, probability of adoptions above threshold is high but less than one. The simulation results show that spread of contagion over $\mathcal{C}_1 \cup \mathcal{G}_{n,1/n}$ is faster than \mathcal{C}_2 when adoptions below threshold happen with probabilities greater than 0.0074. This is consistent with the predictions of Theorem 2, whereby for $\sqrt{n}q \rightarrow \infty$ the time to spread is $O^*(\sqrt{n}/q) = o(n)$ which is strictly faster than $n/2$, the spreading time for complex contagion over \mathcal{C}_2 .

Speed of Complex Contagion with a Few Edges Rewired. In this section, we adopt a more dynamical viewpoint, and interpolate continuously between the random graphs \mathcal{C}_2 and $\mathcal{C}_1 \cup \mathcal{G}_{n,2/n}$. We track the evolution of the spreading time along the interpolation path. Formally, we consider the following continuous time model. Define two random graph processes $\mathcal{D}_\eta, \eta \geq 0$ and $\mathcal{G}_\eta, \eta \geq 0$ that are coupled through the common index $\eta \geq 0$. The coupling is achieved through independent exponential variables that are associated with the edges of the graphs:

- Consider any pair of nodes $i, j \in [n]$. We associate an exponential random variable $X_{ij} > 0$ with mean n^2 to each such pair. Given η , we include edge i, j in random graph \mathcal{G}_η if $X_{ij} < \eta$. Therefore, the random graph \mathcal{G}_η is distributed as Erdős-Rényi with edge probability $\mathbb{P}\{X_{ij} > \eta\} = 1 - e^{-\eta/n^2}$.
- Similarly, with every edge i, j in $\mathcal{C}_2 \setminus \mathcal{C}_1$, we associate an exponential variable Y_{ij} with mean $2n$. For each η , edge i, j is retained in \mathcal{D}_η if $Y_{i,j} > \eta$. Therefore, for each η the probability that the cycle edge i, j is removed is $1 - e^{-\eta/2n}$.

Consider the graph $\mathcal{C}_1 \cup \mathcal{G}_\eta \cup \mathcal{D}_\eta$ in the regime $\eta = o(n)$. Note that for $\eta = o(n)$, the expected degree of nodes in $\mathcal{C}_1 \cup \mathcal{G}_\eta \cup \mathcal{D}_\eta$ is $4 + o(\eta/n)$. Hence, for $\eta = o(n)$ the average degrees

of nodes in $\mathcal{C}_1 \cup \mathcal{G}_\eta \cup \mathcal{D}_\eta$ remains fixed at four, which is the degree of nodes in \mathcal{C}_2 . Motivated by this observation, we refer to $\mathcal{C}_1 \cup \mathcal{G}_\eta \cup \mathcal{D}_\eta$ as the " η -rewired \mathcal{C}_2 " random graph and denote it by \mathcal{C}_2^η . We will use \mathcal{C}_2^η to study what happens as we rewire the $\mathcal{C}_2 \setminus \mathcal{C}_1$ edges. In this context, η denotes the "expected" number of edges that are rewired to construct the random graph \mathcal{C}_2^η from \mathcal{C}_2 .

In the subsequent discussion, we parametrize $\eta = n^\delta$ for $\delta \in (0, 1)$ and study the speed of infection \mathcal{C}_2^η in two regimes:

- (i) For $\delta \in (0, \frac{1}{2})$ we show that the spreading slows down with increasing δ . Hence, rewiring is detrimental to the spread of contagion. In this regime, it is unlikely that two long ties land on the same "faraway" mode. Therefore, complex contagion cannot yet spread through the log-ties when $\delta < 1/2$. In the language of Figure 3, the long-ties are yet too few to form "wide enough bridges" that facilitate the spread of complex contagion. Under such circumstances, the rewiring only slows down the spread, since it introduces new break points for the spread of complex contagion along the cycle edges (short ties).
- (ii) For $\delta \in (\frac{1}{2}, 1)$ we show that contagion takes order $n^{3/2-\delta} + \sqrt{n}/q$ time to spread. For δ large enough, \sqrt{n}/q is the dominant term that fixes the spreading speed. However, for $q \gg 1/\sqrt{n}$ we can specify a range of δ for which increasing δ increases the speed, with complex contagion spreading through the long ties. In particular, if $q = n^{-1/2+\delta'}$, then for $\frac{1}{2} < \delta < \frac{1}{2} + \delta'$ contagion spreads faster in the η -rewired \mathcal{C}_2 .

The following theorem formalizes these intuitions.

Theorem 3 (Rate of 2-complex contagion over \mathcal{C}_2^η with simple adoptions probability q). *Let $\delta \in (0, 1)$, and consider $\eta = n^\delta$:*

- (i) *For fixed $\delta \in (0, \frac{1}{2})$, w.h.p., the total spread time is at least $\frac{n}{2} + \frac{\eta}{4q}$.*
- (ii) *For fixed $\delta \in (\frac{1}{2}, 1)$, the time to global spread can be upper and lower bounded as follows:*
 - (a) *The entire graph is infected by time $4(\sqrt{n}/q + n^{3/2-\delta})(\log \log n)^2$ w.h.p.*
 - (b) *For any $\varepsilon > 0$, the number of infected nodes by time $n^{1/2-\varepsilon}/q$ is at most \sqrt{n} w.h.p.*

In comparison, the time for infection on \mathcal{C}_2 is exactly $n/2$. Thus the first part establishes that for $\eta = o(\sqrt{n})$, the infection spread is slowed down due to the missing edges along the cycle.

Figure 4C shows the spreading time versus the rewiring parameters η for the \mathcal{C}_2^η random graph. It confirms that when the probability of adoptions below threshold q is large enough, the spread of contagions speeds up with the increasing rewiring of the $\mathcal{C}_2 \setminus \mathcal{C}_1$ cycle edges. The plots further verify the theoretical predictions of Theorem 3 about an initial slow down followed by the speeding up of the contagion process as more cycle edges are rewired. In the SI, Figure S2, we include additional simulation results with models that allow for all edges (not just \mathcal{C}_1) to have simple contagion probability q . The additional results demonstrate the same type of qualitative behavior in that rewiring accelerates the spread of complex contagion for large enough q . However, the initial slow down phase that is predicted by Theorem 3 and observed in Figure 4C is not present in Figure S2, where we allow all edges to have simple

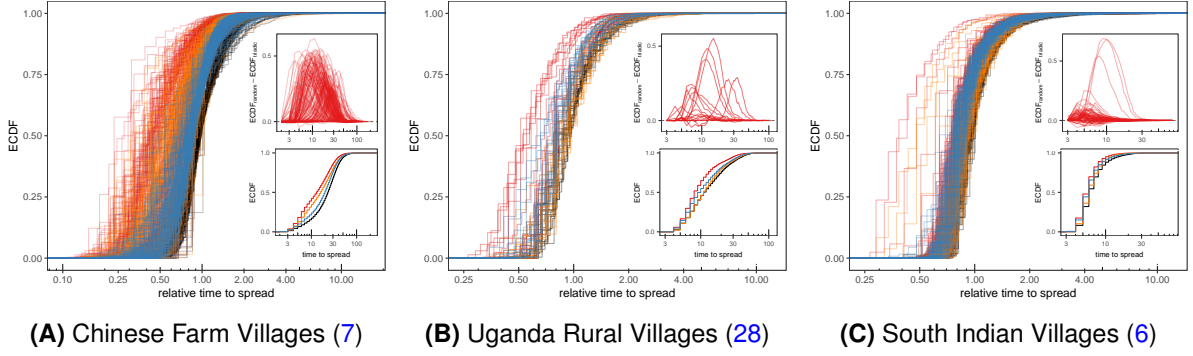


Fig. 6. Speed of complex contagion over empirical social networks with and without interventions that rewire or add edges (using random or triad closing strategies). Each plot in main figures indicate the empirical cumulative distribution function (ECDF) for 500 draws in a particular village social network in the respective dataset. The Chinese farm villages dataset (7) consists of 175 different village networks. For each village in this dataset we plot the ECDF of the spreading times in the original village and under rewiring, as well as random and triad-closing edge additions. Hence, the main figure (A) overlays $4 \times 175 = 700$ plots, corresponding to the ECDFs of the 500 spreading time samples computed for each village under the four conditions: (i) the original villages (no interventions) shown in black, (ii) with 10% of edges rewired shown in orange, (iii) with 10% added edges that are triad-closing shown in blue, and (iv) with 10% new edges added randomly shown in red. Since different networks have different sizes the x-axis is normalized to show the time to spread in proportion to the mean time to spread in the null case (the original network with no interventions), and on a logarithmic scale so as to symmetrize the ratios below and above one. The smaller inset plot at the top shows the difference in ECDFs for each village under random and triad-closing edge additions. The positive difference in each case indicate a case of stochastic dominance: the spreading time over the village network with 10% added triad-closing edges (as a random variable) dominates (is slower than) the spreading time over the network with the 10% new edges added randomly. The smaller inset figure at the bottom combines all the spreading time samples for all villages ($175 \times 500 = 87500$ samples under each of the four conditions) and plots the overall ECDFs for the four conditions (original in black, rewired in orange, triad-closing addition in blue, and random additions in red). Figures (B) and (C) follow the same conventions but their datasets have fewer number of villages. The Ugandan rural villages dataset (28) contains the interconnection data for 17 villages and the south Indian villages dataset contains the interconnection data for 77 villages.

contagion probability q . Indeed, the slow down for $\eta = o(\sqrt{n})$ is an artifact of the handicap that we impose on our model: allowing simple contagion only along the \mathcal{C}_1 edges. Under this handicap restriction, long-ties can facilitate the spread only if they form wide enough bridges for complex contagion to pass (see Figure 3). If the number of rewired edges is too few, $\eta = o(\sqrt{n})$, then the probability that two edges from an infected “island” land on the same faraway node is very small: *the “bridges” are too narrow for complex contagion to pass*. Removing the handicap assumption by allowing simple contagion along all edges (as in Figure S2) will only make our claim stronger: *rewiring accelerates realistic complex contagions even further if we allow simple contagion along the rewired edges*. Our simulations in the next section with other modeling variations, and over empirical network data, verify the robustness of this claim.

Simulations with Empirical Networks. Our theoretical results suggest that replacing short ties with long ties can accelerate the spread of complex contagion in a variety of circumstances.

In this section, we simulate the spread of complex contagion over empirical social networks and measure the time to spread under different hypothetical interventions that rewire or add edges. We analyze the interconnection data from rural Chinese farmers being encouraged to sign up for insurance (7), friendship and health advice networks collected from rural villages in Uganda (28), and multi-dimensional social relations in villages in South India (6). We provide detailed information about these data sets as well as additional analysis for robustness to modeling variations in Supplementary Information Section 6.

In each case, starting from two random seeds (initially infected nodes) we measure the time to 90% spread in the original network and under three interventions: (i) rewiring, (ii) random edge additions, and (iii) edge additions to close open triads. The size of intervention is specified in terms of the percentage of the edges in the original network and we vary them between 5, 10, 15, 20 and 25%. For each type and size, we simulate the spread times over the modified networks 500 times. Figure 6 shows the empirical cumulative distribution functions for the simulated samples in different networks with 10% sized interventions. In these simulations, we fix probability of adoption with a single neighboring adopter at $q = 0.05$. In SI we present a variation of this model where the probability of adoptions above threshold (called ρ) is less than one ($\rho = 0.5, q = 0.025$), as well as a case with very small simple adoption probability ($\rho = 1, q = 0.001$). In another variation, we allow the infected nodes to transition to an inactive state (with probability $\gamma = 0.5$), in which they are no longer infectious, although they are still counted as being infected (adopters). In yet another variation, we consider a fractional threshold model with relative thresholds set to $\theta^* = 0.5$. Simulation results in all cases reveal the same sign and direction for the effect of interventions, although the effect sizes vary. We establish the robustness of our claims to modeling variations as such.

Our simulations indicate that in many real social networks rewiring the edges causes the complex contagion to spread faster. Moreover, contagion spreads faster in the modified network when new edges are added uniformly at random rather than with probability proportional to the number of open triads that they close. The latter has important policy implications: *when proposing new connections to encourage the spread of a behavior over the social network it is beneficial to offer new connections among the long ties*. This is true even if the decisions to adopt rely on local reinforcement from the neighboring adopters (for example with $\rho = 1$ and $q = 0.001$).

Discussion

Contrary to the ideas surrounding the “weakness of long ties”, we find that introduction of long ties and rewiring interventions can accelerate the spread of complex contagion over social networks. In realistic models of complex contagion there is a (small) probability for adoptions to take place even when there is only a single adopter in the social neighborhood. This is enough to change the landscape of results, thereby leading to the conclusion that long ties accelerate these contagions.

For analytical convenience, we studied the 2-complex contagion in a handicapped model where simple adoptions happen only along the cycle edges. We showed that even with the handicap, sub-threshold adoption rates in the order as low as $1/\sqrt{n}$ are enough to induce a faster spread over a rewired network compared to the original structure. Our analysis indicate that the rate of spread over cycle union random graph structures is determined by the time

that it takes for the infected intervals along the cycle to grow long enough, to makes the spread of complex contagion through their long ties a probable event. This idea is reasonably general and can be applied to modeling variations where complex contagions happen with a probability less than one ($\rho < 1$) or the adoption thresholds are greater than two ($\theta > 2$). In both cases the spread will be slowed down either to wait for the complex contagions to occur at the slower $1/\rho$ rate or for the intervals to grow longer to make a more stringent θ -complex adoption probable. We test these results on real network data and measure the speed of spread under various structural interventions. Our numerical results on real networks are aligned with the theoretical findings. In particular, we find that addition of long ties lead to faster spread compared to closing triads.

Our results indicate that introduction of long ties are more effective for accelerating the spread of social contagion. Thereby we propose a more unified recommendation for structural interventions by inclusion of long ties in less clustered neighborhoods to cause a faster spread. This is consistent with empirical studies that identify structural diversity as an indicator of increased adoption (4). However, structural interventions in networks usually happen through recommendations that suggest potential new connections to the users, and the decision to form a tie is often correlated with the adoption decisions. Individuals have varying tendencies for accepting new ties that are suggested to them and these tendencies may affect their adoption decisions as well. Our results do not address the decision to form a tie or how the latter is correlated with the subsequent adoption decisions. Rather, we clarify the effect that the introduction of new ties has on the speed of spread. We propose the confluence of these two decisions — whether to form a tie and whether to adopt a behavior given the status of people with whom one has formed a tie — as a topic for a future study.

Materials and Methods

The data for the simulation studies are derived from (6, 7, 28) which are publicly available (online). Code for reported simulations can be accessed from <https://github.com/aminrahimian/social-contagion/wiki>.

ACKNOWLEDGMENTS. E.M. is partially supported by NSF grant CCF 1665252, DOD ONR grant N00014-17-1-2598, and NSF grant DMS- 1737944.

1. Jones GE (1963) The diffusion of agricultural innovations. *Journal of Agricultural Economics* 15(3):387–409.
2. Rogers EM (2003) *Diffusion of Innovations*. (Simon and Schuster), 5 edition.
3. Beaman L, BenYishay A, Magruder J, Mobarak AM (2018) Can network theory-based targeting increase technology adoption?, (National Bureau of Economic Research), Technical Report 24912.
4. Ugander J, Backstrom L, Marlow C, Kleinberg J (2012) Structural diversity in social contagion. *Proceedings of the National Academy of Sciences* 109(16):5962–5966.
5. Iyengar R, Van den Bulte C, Valente TW (2011) Opinion leadership and social contagion in new product diffusion. *Marketing Science* 30(2):195–212.
6. Banerjee A, Chandrasekhar AG, Duflo E, Jackson MO (2013) The diffusion of microfinance. *Science* 341(6144):1236498.
7. Cai J, De Janvry A, Sadoulet E (2015) Social networks and the decision to insure. *American Economic Journal: Applied Economics* 7(2):81–108.
8. Eckles D, Kizilcec RF, Bakshy E (2016) Estimating peer effects in networks with peer encouragement designs. *Proceedings of the National Academy of Sciences* 113(27):7316–7322.
9. Wu J, Crawford FW, Kim DA, Stafford D, Christakis NA (2018) Exposure, hazard, and survival analysis of diffusion on social networks. *Statistics in Medicine* 37(17):2561–2585.

10. Nickerson DW (2008) Is voting contagious? Evidence from two field experiments. *American Political Science Review* 102(1):49–57.
11. Bond RM, et al. (2012) A 61-million-person experiment in social influence and political mobilization. *Nature* 489(7415):295–298.
12. Jones JJ, Bond RM, Bakshy E, Eckles D, Fowler JH (2017) Social influence and political mobilization: Further evidence from a randomized experiment in the 2012 US Presidential Election. *PLOS ONE* 12(4):e0173851.
13. Aral S, Nicolaides C (2017) Exercise contagion in a global social network. *Nature Communications* 8.
14. Friggeri A, Adamic LA, Eckles D, Cheng J (2014) Rumor cascades in *Proceedings of ICWSM*. (AAAI).
15. Vosoughi S, Roy D, Aral S (2018) The spread of true and false news online. *Science* 359(6380):1146–1151.
16. Gray V (1973) Innovation in the states: A diffusion study. *American Political Science Review* 67(4):1174–1185.
17. Balla SJ (2001) Interstate professional associations and the diffusion of policy innovations. *American Politics Research* 29(3):221–245.
18. Whiten A, Horner V, De Waal FB (2005) Conformity to cultural norms of tool use in chimpanzees. *Nature* 437(7059):737–740.
19. Allen J, Weinrich M, Hoppitt W, Rendell L (2013) Network-based diffusion analysis reveals cultural transmission of lottail feeding in humpback whales. *Science* 340(6131):485–488.
20. van de Waal E, Borgeaud C, Whiten A (2013) Potent social learning and conformity shape a wild primate's foraging decisions. *Science* 340(6131):483–485.
21. Aplin LM, et al. (2015) Experimentally induced innovations lead to persistent culture via conformity in wild birds. *Nature* 518(7540):538–541.
22. Leskovec J, Adamic LA, Huberman BA (2007) The dynamics of viral marketing. *ACM Transactions on the Web (TWEB)* 1(1):5.
23. Kempe D, Kleinberg J, Tardos É (2003) Maximizing the spread of influence through a social network in *Proceedings of the ninth ACM SIGKDD international conference on Knowledge discovery and data mining*. (ACM), pp. 137–146.
24. Hinz O, Skiera B, Barrot C, Becker JU (2011) Seeding strategies for viral marketing: An empirical comparison. *Journal of Marketing* 75(6):55–71.
25. Libai B, Muller E, Peres R (2013) Decomposing the value of word-of-mouth seeding programs: Acceleration versus expansion. *Journal of Marketing Research* 50(2):161–176.
26. Cohen R, Havlin S, Ben-Avraham D (2003) Efficient immunization strategies for computer networks and populations. *Physical Review Letters* 91(24):247901.
27. Preciado VM, Zargham M, Enyioha C, Jadbabaie A, Pappas GJ (2014) Optimal resource allocation for network protection against spreading processes. *IEEE Transactions on Control of Network Systems* 1(1):99–108.
28. Chami GF, Ahnert SE, Kabatereine NB, Tukahebwa EM (2017) Social network fragmentation and community health. *Proceedings of the National Academy of Sciences* 114(36):E7425–E7431.
29. Chaoji V, Ranu S, Rastogi R, Bhatt R (2012) Recommendations to boost content spread in social networks in *Proceedings of the 21st international conference on World Wide Web*. (ACM), pp. 529–538.
30. Valente TW (2012) Network interventions. *Science* 337(6090):49–53.
31. Carrell SE, Sacerdote BI, West JE (2013) From natural variation to optimal policy? The importance of endogenous peer group formation. *Econometrica* 81(3):855–882.
32. Cerdeiro DA, Dziubiński M, Goyal S (2017) Individual security, contagion, and network design. *Journal of Economic Theory* 170:182–226.
33. Dodds PS, Watts DJ (2005) A generalized model of social and biological contagion. *Journal of Theoretical Biology* 232(4):587–604.
34. Hébert-Dufresne L, Noël PA, Marceau V, Allard A, Dubé LJ (2010) Propagation dynamics on networks featuring complex topologies. *Physical Review E* 82(3):036115.
35. Volz EM, Miller JC, Galvani A, Meyers LA (2011) Effects of heterogeneous and clustered contact patterns on infectious disease dynamics. *PLoS Computational Biology* 7(6):e1002042.
36. Granovetter MS (1973) The strength of weak ties. *American journal of sociology* 78(6):1360–1380.
37. Gee LK, Jones JJ, Fariss CJ, Burke M, Fowler JH (2017) The paradox of weak ties in 55 countries. *Journal of Economic Behavior & Organization* 133:362–372.

38. Burt RS (1987) Social contagion and innovation: Cohesion versus structural equivalence. *American journal of Sociology* 92(6):1287–1335.
39. Aral S, Van Alstyne M (2011) The diversity-bandwidth trade-off. *American Journal of Sociology* 117(1):90–171.
40. Granovetter M (1978) Threshold models of collective behavior. *American journal of sociology* 83(6):1420–1443.
41. Centola D, Macy M (2007) Complex contagions and the weakness of long ties. *American journal of Sociology* 113(3):702–734.
42. Galeotti A, Goyal S, Jackson MO, Vega-Redondo F, Yariv L (2010) Network games. *The Review of Economic Studies* 77(1):218–244.
43. Blume LE (1993) The statistical mechanics of strategic interaction. *Games and Economic Behavior* 5(3):387–424.
44. Morris S (2000) Contagion. *The Review of Economic Studies* 67(1):57–78.
45. Young HP (2011) The dynamics of social innovation. *Proceedings of the National Academy of Sciences* 108(Supplement 4):21285–21291.
46. Montanari A, Saberi A (2010) The spread of innovations in social networks. *Proceedings of the National Academy of Sciences* 107(47):20196–20201.
47. Nematzadeh A, Ferrara E, Flammini A, Ahn YY (2014) Optimal network modularity for information diffusion. *Physical review letters* 113(8):088701.
48. Hébert-Dufresne L, Althouse BM (2015) Complex dynamics of synergistic coinfections on realistically clustered networks. *Proceedings of the National Academy of Sciences* 112(33):10551–10556.
49. Bakshy E, Rosenn I, Marlow C, Adamic L (2012) The role of social networks in information diffusion in *Proceedings of the 21st international conference on World Wide Web*. (ACM), pp. 519–528.
50. Bakshy E, Eckles D, Yan R, Rosenn I (2012) Social influence in social advertising: evidence from field experiments in *Proceedings of the 13th ACM conference on electronic commerce*. (ACM), pp. 146–161.
51. Centola D (2010) The spread of behavior in an online social network experiment. *Science* 329(5996):1194–1197.
52. Janson S, Kozma R, Ruzinkó M, Sokolov Y (2016) Bootstrap percolation on a random graph coupled with a lattice. *Electronic Journal of Combinatorics*.
53. Durrett R (2010) Some features of the spread of epidemics and information on a random graph. *Proceedings of the National Academy of Sciences*.
54. Ghasemiesfeh G, Ebrahimi R, Gao J (2013) Complex contagion and the weakness of long ties in social networks: revisited in *Proceedings of the fourteenth ACM conference on Electronic Commerce*. (ACM), pp. 507–524.
55. Ebrahimi R, Gao J, Ghasemiesfeh G, Schoenebeck G (2015) Complex contagions in kleinberg's small world model in *Proceedings of the 2015 Conference on Innovations in Theoretical Computer Science*. (ACM), pp. 63–72.
56. Ebrahimi R, Gao J, Ghasemiesfeh G, Schoenebeck G (2017) How complex contagions spread quickly in preferential attachment models and other time-evolving networks. *IEEE Transactions on Network Science and Engineering* 4(4):201–214.
57. Schoenebeck G, Yu FY (2016) Complex contagions on configuration model graphs with a power-law degree distribution in *International Conference on Web and Internet Economics*. (Springer), pp. 459–472.
58. Jackson MO, Yariv L (2007) Diffusion of behavior and equilibrium properties in network games. *American Economic Review* 97(2):92–98.
59. Acemoglu D, Ozdaglar A, Yildiz E (2011) Diffusion of innovations in social networks in *Decision and Control and European Control Conference (CDC-ECC), 2011 50th IEEE Conference on*. (IEEE), pp. 2329–2334.
60. Watts DJ, Strogatz SH (1998) Collective dynamics of 'small-world' networks. *nature* 393(6684):440.
61. Newman ME, Watts DJ (1999) Renormalization group analysis of the small-world network model. *Physics Letters A* 263(4-6):341–346.
62. Balogh J, Pittel BG (2007) Bootstrap percolation on the random regular graph. *Random Structures & Algorithms* 30(1-2):257–286.
63. Amini H, Fountoulakis N (2014) Bootstrap percolation in power-law random graphs. *Journal of Statistical*

- Physics* 155(1):72–92.
64. Amini H (2010) Bootstrap percolation and diffusion in random graphs with given vertex degrees. *the electronic journal of combinatorics* 17(1):25.
 65. Newman ME, Watts DJ (1999) Scaling and percolation in the small-world network model. *Physical review E* 60(6):7332.

Supplementary Information for

Long ties accelerate noisy threshold-based contagions

Dean Eckles, Elchanan Mossel, M. Amin Rahimian and Subhabrata Sen

E-mails:{eckles,elmos,rahimian,ssen90}@mit.edu

This PDF file includes:

Supplementary text
Figs. S1 to S7
References for SI reference citations

Supporting Information Text

This Supplementary Information is organized in four sections that parallel the four parts of the Results section in the main text. Sections 1, 2, and 3 include the proofs for Theorems 1, 2 and 3 from the main text, as well as additional simulations. In Section 4, we expand on our study of empirical networks and present additional simulation results under various contagion models that deviate from those considered in the main text. These additional results support the robustness of our claims against modeling variations.

Notation: For convenience of the reader, we collect here some notation that will be used throughout in the subsequent discussion. For sequences of real numbers, we use the usual Bachman-Landau notation $O(\cdot)$, $o(\cdot)$ and $\Theta(\cdot)$. Further, for a sequence of non-negative real numbers $\{a_n : n \geq 1\}$ and a sequence of random variables $\{X_n : n \geq 1\}$, we say that $X_n = o(a_n)$ if $X_n/a_n \xrightarrow{P} 0$ as $n \rightarrow \infty$. Similarly, we declare $X_n = O(a_n)$ if there exists a universal constant $C > 0$ such that $\mathbb{P}(|X_n|/a_n \leq C) \rightarrow 1$ as $n \rightarrow \infty$. Finally, say that $X_n = \Theta(a_n)$ if there exist universal constants $0 < c < C < \infty$ such that $\mathbb{P}(ca_n < X_n < Ca_n) \rightarrow 1$ as $n \rightarrow \infty$. For two random variables X, Y , we set $X \preceq Y$ if X is stochastically dominated by Y . A sequence of events $\{A_n\}$ occurs with high probability as $n \rightarrow \infty$ (referred to as w.h.p.) if $\mathbb{P}(A_n^c) \rightarrow 0$ as $n \rightarrow \infty$.

1. Spread of complex contagion over \mathcal{C}_2 union random graphs (Theorem 1)

In this section we provide the asymptotic rate of 2-complex contagion over $\mathcal{C}_2 \cup \mathcal{G}_{n,c/n}$, and compare it with $\mathcal{C}_{2+c/2}$. We conclude that the diffusion speed is faster in the rewired graph. Therefore, we emphasize the understanding that rewiring facilitates the spread of complex contagion as long as the required structure for total spread (\mathcal{C}_2) is intact.

A. Speed lower-bound for complex contagion.

Theorem 1.1 (Upper-Bounding the number of infected nodes until $t = o(n^{3/4})$). *Let I_t denote the number of infected nodes at time t . For $t = o(n^{3/4})$, $I_t = o(n^{3/4})$.*

Proof. Let \mathcal{I}_t be the set of all infected nodes at time t and let \mathcal{B}_t denote the interval of length $2t$ from the deterministic growth of the two neighboring initial seeds: $B_t = |\mathcal{B}_t| = 2t = T$. Note that the vertices in \mathcal{B}_t are always infected due to two-complex contagion along \mathcal{C}_2 . We define $\mathcal{I}_t^0 = \mathcal{B}_t$ and note that $\mathcal{I}_t^0 \subset \mathcal{I}_t$. However, other vertices might be infected due to complex contagion along the edges of $\mathcal{G}_{n,c/n}$. To control these secondary infections, we introduce an algorithm which proceeds in rounds, and builds up the infected set $\{I_t^\tau : \tau \geq 1\}$ by exposing new random edges connecting currently infected vertices to “healthy”-vertices. The analysis below tracks the growth of the infected set over iterations, and establishes that for $t = o(n^{3/4})$, the algorithm terminates in four rounds with high probability. Further, the additional infected vertices gained are $o(n^{3/4})$ in number, and all isolated. Thus they do not give rise to secondary infections along \mathcal{C}_2 via 2-complex contagion.

Let us introduce the sequential algorithm formally before we proceed further. For notational convenience, let $\{S_t^\tau : \tau \geq 1\}$ denote nodes with exactly one neighbor in \mathcal{I}_t^τ and call them “susceptible” nodes. Further, let \mathcal{H}_t^τ denote nodes that have no neighbors in \mathcal{I}_t^τ and call them “healthy” nodes. Moreover, we denote the nodes that join the infected set at step τ by $\mathcal{A}_t^\tau = \mathcal{I}_t^\tau \setminus \mathcal{I}_t^{\tau-1}$. Finally, for $v \in [n]$ and $C \subset [n]$, $\mathcal{N}_C(v)$ will denote the number of neighbors of v in the set C .

Algorithm: Edge-Revelation

- Initialize:
 - $\mathcal{I}_t^0 = \mathcal{B}_t$, $\mathcal{A}_t^0 = \mathcal{B}_t$, $\mathcal{S}_t^0 = \emptyset$, $\mathcal{H}_t^0 = [n] \setminus (\mathcal{I}_t^0 \cup \mathcal{S}_t^0)$.
- For $\tau \geq 1$, given $(\mathcal{I}_t^{\tau-1}, \mathcal{A}_t^{\tau-1}, \mathcal{S}_t^{\tau-1}, \mathcal{H}_t^{\tau-1})$:
 - Reveal all the long ties that are incident to $\mathcal{A}_t^{\tau-1}$.
 - Update the sets using the revealed edges:
 - * $\bar{\mathcal{S}}_t^\tau = \{v \in \mathcal{S}_t^{\tau-1} : \mathcal{N}_{\mathcal{I}_t^{\tau-1} \setminus \mathcal{I}_t^{(\tau-2)}}(v) \geq 1\}$.
These are the susceptible vertices that join the infected set at step τ .
 - * $\bar{\mathcal{H}}_t^\tau = \{v \in \mathcal{H}_t^{\tau-1} : \mathcal{N}_{\mathcal{I}_t^{\tau-1} \setminus \mathcal{I}_t^{(\tau-2)}}(v) \geq 2\}$.
These are the healthy vertices that join the infected set at step τ .
 - * $\hat{\mathcal{H}}_t^\tau = \{v \in \mathcal{H}_t^{\tau-1} : \mathcal{N}_{\mathcal{I}_t^{\tau-1}}(v) = 1\} = \{v \in \mathcal{H}_t^{\tau-1} : \mathcal{N}_{\mathcal{I}_t^{\tau-1} \setminus \mathcal{I}_t^{\tau-2}}(v) = 1\}$.
These are the healthy vertices that join the susceptible set at step τ .
 - * $\mathcal{A}_t^\tau = \bar{\mathcal{S}}_t^\tau \cup \bar{\mathcal{H}}_t^\tau$, these are the nodes that become infected in step τ .
 - * $\mathcal{I}_t^\tau = \mathcal{I}_t^{\tau-1} \cup \mathcal{A}_t^\tau$, adding the nodes that become infected in step τ .
 - * $\mathcal{S}_t^\tau = \mathcal{S}_t^{\tau-1} \cup \hat{\mathcal{H}}_t^\tau \setminus \bar{\mathcal{S}}_t^\tau$, updating the set of susceptible nodes for step $\tau + 1$.
 - * $\mathcal{H}_t^\tau = \mathcal{H}_t^{\tau-1} \setminus (\bar{\mathcal{H}}_t^\tau \cup \hat{\mathcal{H}}_t^\tau)$, updating the set of healthy nodes for the next step.

The algorithm terminates at the first step $\tau \geq 1$, such that $\bar{\mathcal{S}}_t^\tau \cup \bar{\mathcal{H}}_t^\tau = \emptyset$. Upon termination at τ , we have that $\mathcal{I}_t^\tau = \mathcal{I}_t$. We show that when $t = o(n^{3/4})$, then with high probability this algorithm terminates in $\tau = 4$; moreover, $I_t = I_t^{(4)} = o(n^{3/4})$ w.h.p. For notational convenience, we use roman fonts to refer to sizes of sets introduced in the Edge-Revelation algorithm introduced above— for example, $H_t^0 = |\mathcal{H}_t^0|$, $B_t = |\mathcal{B}_t|$ and so on. We will refer to the natural filtration associated with this sequential procedure as $\{\mathcal{F}_\tau : \tau \geq 1\}$.

We analyze the rounds of the algorithm sequentially. We start with $\tau = 0$, and note that $I_t^0 = B_t = 2t = T = o(n^{3/4})$. For $\tau = 1$, we get:

$$\begin{aligned}\hat{H}_t^1 &= \text{Bin}(H_t^0, \mathbb{P}[\text{Bin}(A_t^0, c/n) = 1]) \\ \bar{H}_t^1 &= \text{Bin}(2t, \mathbb{P}[\text{Bin}(A_t^0, c/n) = 1]) + \text{Bin}(H_t^0, \mathbb{P}[\text{Bin}(A_t^0, c/n) \geq 2]) \\ \bar{S}_t^1 &= \text{Bin}(S_t^0, \mathbb{P}[\text{Bin}(A_t^0, c/n) \geq 1]) = 0.\end{aligned}$$

Direct computation yields $\mathbb{E}[\hat{H}_t^1] = o(n^{3/4})$ and $\mathbb{E}[\bar{H}_t^1] = o(\sqrt{n})$. Using Markov inequality, this immediately implies that $\hat{H}_t^1 = o(n^{3/4})$ and $\bar{H}_t^1 = o(\sqrt{n})$. This, in turn implies that

$$\begin{aligned}S_t^1 &= S_t^0 - \bar{S}_t^1 + \hat{H}_t^1 = T = o(n^{3/4}), \quad H_t^1 = H_t^0 - \bar{H}_t^1 - \hat{H}_t^1 = \Theta(n), \\ A_t^1 &= \bar{H}_t^1 = o(\sqrt{n}), \quad I_t^1 = I_t^0 + A_t^1 = o(n^{3/4}).\end{aligned}$$

We next analyze the next round of the Edge Revelation algorithm. For $\tau = 2$, we have

$$\begin{aligned}\hat{H}_t^2 &= \text{Bin}(H_t^1, \mathbb{P}[\text{Bin}(A_t^1, c/n) = 1]) \\ \bar{H}_t^2 &= \text{Bin}(H_t^1, \mathbb{P}[\text{Bin}(A_t^1, c/n) \geq 2]) \\ \bar{S}_t^2 &= \text{Bin}(S_t^1, \mathbb{P}[\text{Bin}(A_t^1, c/n) \geq 1]).\end{aligned}$$

For any $\varepsilon > 0$, we have, for $\delta_1, \delta_2 > 0$

$$\begin{aligned}\mathbb{P}[\hat{H}_t^2 > \varepsilon\sqrt{n}] &\leq \mathbb{P}[\hat{H}_t^2 > \varepsilon\sqrt{n}, H_t^1 < \delta_1 n, A_t^1 < \delta_2\sqrt{n}] + o(1) \\ &\leq \frac{\delta_1\delta_2}{\varepsilon} + o(1),\end{aligned}$$

where the last inequality follows using Markov inequality, conditioned on \mathcal{F}_1 . We note that as $\delta_1, \delta_2 > 0$ are arbitrary, $\hat{H}_t^2 = o(\sqrt{n})$. A similar analysis reveals that $\bar{H}_t^2 = o(1)$ and $\bar{S}_t^2 = o(n^{1/4})$. Armed with these observations, we immediately conclude that

$$\begin{aligned}S_t^2 &\leq 4A_t^1 + S_t^1 - \bar{S}_t^2 + \hat{H}_t^2 = o(n^{3/4}), \quad H_t^2 = H_t^1 - \bar{H}_t^2 - \hat{H}_t^2 = \Theta(n), \\ A_t^2 &= \bar{S}_t^2 + \bar{H}_t^2 = o(n^{1/4}), \quad I_t^2 = I_t^1 + A_t^2 = o(n^{3/4}).\end{aligned}$$

The same recursion continue to hold for $\tau = 3, 4$:

$$\begin{aligned}
\hat{H}_t^\tau &= \text{Bin}(H_t^{\tau-1}, \mathbb{P}[\text{Bin}(A_t^{\tau-1}, c/n) = 1]) \\
\bar{H}_t^\tau &= \text{Bin}(H_t^{\tau-1}, \mathbb{P}[\text{Bin}(A_t^{\tau-1}, c/n) \geq 2]) \\
\bar{S}_t^\tau &= \text{Bin}(S_t^{\tau-1} - 2, \mathbb{P}[\text{Bin}(A_t^{\tau-1}, c/n) \geq 1]) \\
S_t^\tau &\leq 4A_t^\tau + S_t^{\tau-1} - \bar{S}_t^\tau + \hat{H}_t^\tau, \quad H_t^\tau = H_t^{\tau-1} - \bar{H}_t^{\tau-1} - \hat{H}_t^{\tau-1}, \\
A_t^\tau &= \bar{S}_t^\tau + \bar{H}_t^\tau, \quad I_t^\tau = I_t^{\tau-1} + A_t^{\tau-1}.
\end{aligned} \tag{1}$$

The upper-bound in [1] is due to the $4A_t^\tau$ term which accounts for the four neighbors of an additionally infected node (outside of \mathcal{B}_t) on the \mathcal{C}_2 . The validity of this recursion hinges crucially on the observation that with high probability, two infected nodes do not occur next to each other. We state this assertion formally in the lemma below, and complete the proof assuming the lemma below. We defer its proof to the end of the section.

Lemma 1.2. *With high probability as $n \rightarrow \infty$, for $1 \leq \tau \leq 4$, no two infected vertices outside \mathcal{B}_t are adjacent.*

To track the evolution of the infected and susceptible vertices over the subsequent iterations of the Edge-Revelation algorithm, we make the following elementary observation. For any sequence $a_n = o(n)$, on the event $\{A_t^{\tau-1} \leq a_n\}$, we have, using Taylor expansion for the binomial probabilities:

$$\begin{aligned}
\mathbb{P}[\text{Bin}(A_t^{\tau-1}, c/n) \geq 1 \mid \mathcal{F}_{\tau-1}] &= 1 - (1 - \frac{c}{n})^{A_t^{\tau-1}} = 1 - \left(1 - A_t^{\tau-1} \frac{c}{n} + O\left(\frac{(cA_t^{\tau-1})^2}{n^2}\right)\right) \\
&= (1 + o(1))A_t^{\tau-1} \frac{c}{n}.
\end{aligned}$$

Similarly, on the event $\{A_t^{\tau-1} \leq a_n\}$,

$$\begin{aligned}
&\mathbb{P}[\text{Bin}(A_t^{\tau-1}, c/n) \geq 2 \mid \mathcal{F}_{\tau-1}] \\
&= 1 - (1 - \frac{c}{n})^{A_t^{\tau-1}} - \frac{c}{n} A_t^{\tau-1} (1 - \frac{c}{n})^{A_t^{\tau-1}-1} \\
&= 1 - \left(1 - A_t^{\tau-1} \frac{c}{n} + \frac{c^2}{2n^2} (A_t^{\tau-1})(A_t^{\tau-1} - 1) + o\left(\frac{(cA_t^{\tau-1})^2}{n^2}\right)\right) \\
&\quad - \frac{c}{n} A_t^{\tau-1} \left(1 - (A_t^{\tau-1} - 1) \frac{c}{n} + O\left(\frac{(cA_t^{\tau-1})^2}{n^2}\right)\right) \\
&= (1 + o(1)) \left(\frac{(cA_t^{\tau-1})^2}{2n^2}\right).
\end{aligned}$$

The following table summarizes the evolution of the Edge-Revelation algorithm at steps $\tau = 0, 1, 2, 3, 4$. These properties are derived by analogous computations as those for $\tau = 2$.

	$\tau = 0$	$\tau = 1$	$\tau = 2$	$\tau = 3$	$\tau = 4$
\hat{H}_t^τ	0	$o(n^{3/4})$	$o(\sqrt{n})$	$o(n^{1/4})$	$o(1)$
\bar{H}_t^τ	0	$o(\sqrt{n})$	$o(1)$	$o(n^{-1/2})$	$o(n^{-1})$
\bar{S}_t^τ	0	0	$o(n^{1/4})$	$o(1)$	$o(n^{-1/4})$
S_t^τ	2	$o(n^{3/4})$	$o(n^{3/4})$	$o(n^{3/4})$	$o(n^{3/4})$
H_t^τ	$\Theta(n)$	$\Theta(n)$	$\Theta(n)$	$\Theta(n)$	$\Theta(n)$
A_t^τ	$o(n^{3/4})$	$o(\sqrt{n})$	$o(n^{1/4})$	$o(1)$	$o(n^{-1/4})$
I_t^τ	$o(n^{3/4})$	$o(n^{3/4})$	$o(n^{3/4})$	$o(n^{3/4})$	$o(n^{3/4})$

Note that after $\tau = 3$ steps the algorithm terminates with high probability, as there are no additional infected nodes identified. At each step the number of additional infected nodes that are identified (A_t^τ) is reduced by a factor of $n^{-1/4}$. During these four steps the total number of infected nodes that have been identified remains $o(n^{3/4})$ with high probability. This completes the proof. \square

Finally, we turn to the proof of Lemma 1.2.

Proof of Lemma 1.2: We seek to prove that the edge-revelation algorithm does not create a pair of adjacent infected nodes in the first four rounds with high probability. To establish that this “good” event holds with high probability, fix $1 \leq \tau \leq 4$, and consider the various possible states of adjacent node pairs after $\tau - 1$ rounds of the edge revelation algorithm. For ease of notation, we refer to the elements of $\mathcal{I}_t^{\tau-1}$, $\mathcal{S}_t^{\tau-1}$, and $\mathcal{H}_t^{\tau-1}$ as \mathcal{H} -nodes, \mathcal{S} -nodes, and \mathcal{I} -nodes, respectively. At step $\tau \leq 4$, two neighboring infected nodes can appear if the revealed edges are incident to one of the following category of pairs:

- a pair of adjacent \mathcal{H} -nodes.
- a pair of adjacent \mathcal{H} and \mathcal{S} nodes.
- a pair of adjacent \mathcal{H} and \mathcal{I} nodes.
- a pair of adjacent \mathcal{I} and \mathcal{S} nodes.
- a pair of adjacent \mathcal{S} nodes.

At any step $1 \leq \tau \leq 4$, denote the number of pairs in each category above by HH_t^τ , SH_t^τ , HI_t^τ , IS_t^τ , SS_t^τ respectively. We have,

$$HH_t^\tau \leq H_t^\tau = \Theta(n), SH_t^\tau \leq S_t^\tau = o(n^{3/4}), HI_t^\tau \leq I_t^\tau - I_t^0 = o(\sqrt{n}), \quad [2]$$

$$IS_t^\tau \leq 2 + I_t^\tau - I_t^0 = 2\mathbb{1}_{\{\tau=0\}} + o(\sqrt{n})\mathbb{1}_{\{\tau>0\}}, SS_t^\tau \leq S_t^\tau = 2\mathbb{1}_{\{\tau=0\}} + \mathbb{1}_{\{\tau>0\}}o(n^{3/4}) \quad [3]$$

Next, we track the actual number of infected consecutive node pairs appearing from each category. To this end, we denote these numbers as $\Pi(\cdot)$ respectively.

Note that $\Pi(HH_t^\tau) = \sum_{j=1}^{HH_t^\tau} I_j$, where I_j indicates whether the i^{th} $\mathcal{H}\mathcal{H}_t^\tau$ pair is infected as a result of the edge revelation algorithm. Observe that given $\mathcal{F}_{\tau-1}$, $\mathbb{P}[I_j = 1] = (\mathbb{P}[\text{Bin}(A_t^\tau, c/n) \geq 2])^2$. Thus we have,

$$\mathbb{E}[\Pi(HH_t^\tau) | \mathcal{F}_{\tau-1}] = HH_t^\tau (\mathbb{P}[\text{Bin}(A_t^\tau, c/n) \geq 2])^2.$$

We can control $\mathbb{P}[\text{Bin}(A_t^\tau, c/n) \geq 2]$ using [2]. Further, using the table above and [3] coupled with Markov inequality, we conclude that $\Pi(HH_t^\tau) = o(1)$. The control of the other terms is similar, and thus we omit detailed computations, and only describe the relevant modifications. To analyze $\Pi(SH_t^\tau)$, note that given $\mathcal{F}_{\tau-1}$, $\Pi(SH_t^\tau)$ is expressed as a sum of SH_t^τ independent indicators with probability $\mathbb{P}[\text{Bin}(A_t^{\tau-1}, c/n) \geq 1] \mathbb{P}[\text{Bin}(A_t^\tau, c/n) \geq 2]$. As before, we control the probability using Taylor expansion and the table above, and control the number of trials using [3]. Finally, Markov inequality immediately implies that $\Pi(SH_t^\tau) = o(1)$. In case of $\Pi(HI_t^\tau)$, the conditional probability of contribution of each pair, given $\mathcal{F}_{\tau-1}$, is $\mathbb{P}[\text{Bin}(A_t^\tau, c/n) \geq 2]$. The relevant probabilities for $\Pi(IS_t^\tau)$, $\Pi(SS_t^\tau)$ are $\mathbb{P}[\text{Bin}(A_t^\tau, c/n) \geq 1]$ and $\mathbb{P}[\text{Bin}(A_t^\tau, c/n) \geq 1]^2$ respectively. The rest of the argument is exactly same, and implies that for $\tau \leq 4$, each term is $o(1)$ as $n \rightarrow \infty$. This completes the proof. \square

B. Speed Upper-Bound for Complex Contagion.

Theorem 1.3. *With high probability, the entire graph will be infected in time $n^{3/4}(\log \log n)^2(1 + o(1))$.*

Proof of Theorem 1.3. We devise an algorithm to lower bound the initial growth of the set of infected nodes. Let us consider a sequence $a_n \rightarrow \infty$ as $n \rightarrow \infty$, to be specified later. Next, we divide the cycle into consecutive intervals of length $L = n^{3/4}a_n(\log \log n)^2$. Call an interval *active* if two neighboring nodes (an adjacent pair) within that interval are infected. Initially, declare the interval containing the original seed nodes as an active interval. Starting with the initial seed nodes, after $n^{3/4}a_n$ steps the length of the original interval grows to $2n^{3/4}a_n$. In general, after $n^{3/4}a_n$ time steps the length of infected segments in each active interval will be at least $n^{3/4}a_n$ due to the deterministic growth along the cycle. By revealing the edges of $\mathcal{G}_{n,c/n}$ that are incident to the newly infected nodes at the end of each $n^{3/4}a_n$ epoch, we can identify new active intervals that will, in turn, grow and activate other intervals. Formally, we consider the following algorithm to undercount the number of infected nodes. Denote by X_τ the number of active intervals after τ epochs of length $n^{3/4}a_n$.

Algorithm: Interval-Growth

- Initialize:
 - Let $N = n/L = n^{1/4}/(a_n(\log \log n)^2)$. Divide the cycle into N intervals of length L each, and label them by $[N]$; let the initial seed nodes be contained in the interval that is labeled one: $\mathcal{X}_0 = \{1\}$.
- For $\tau \geq 1$, given $\mathcal{X}_{\tau-1}$:
 - Infect $n^{3/4}a_n$ new nodes along the cycle in each of the active intervals. Add edges independently with probability c/n , connecting the newly infected nodes to the healthy nodes.
 - Update the set of active intervals by adding all intervals that have two adjacent infected nodes due to the edge exposure operation in the previous step: $\mathcal{X}_\tau \leftarrow \mathcal{X}_{\tau-1}$.

The following lemma derives a lower bound on the number of active intervals after $O(\log \log n)$ steps.

Lemma 1.4 (Initial Growth of the intervals). *For any $C > 0$, there exists a sequence $t_n := t_n(C) = o(\log \log n)$ such that for*

$$\tau_n = \frac{1}{\log 4} \left(\log \log n + t_n \right),$$

with high probability as $n \rightarrow \infty$, $X_{\tau_n} \geq Cn^{1/16}(\log n)^{1/4}$.

An extra $n^{3/4}$ epoch beyond τ_n ensures that each activated interval has at least $n^{3/4}$ infected nodes. The next Lemma shows that this is enough to guarantee that the whole graph will be infected in $(\tau_n + 2)n^{3/4}$ time.

Lemma 1.5 (End Regime). *Let T_n be the first time that 2-complex contagion infects $Cn^{3/4+1/16}(\log n)^{1/4}$ nodes, where $C > 2/c$ is a universal constant. Then with high probability, all nodes are infected by time $T_n + n^{3/4} + 1$.*

This concludes the proof. \square

It remains to prove Lemma 1.4 and Lemma 1.5. We first turn to the proof of Lemma 1.4.

Proof of Lemma 1.4. Let us denote the natural filtration associated with this growth process as $\{\mathcal{F}_\tau : \tau \geq 1\}$. Note that at the end of $\tau - 1$ steps, we have $X_{\tau-1}$ infected intervals, and thus $N - X_{\tau-1}$ non-active intervals. Each non-active interval of length L has at least $\frac{1}{2}L$ mutually disjoint adjacent pairs, and the interval is activated if any one of these adjacent pairs is infected by the next step of the Interval-Growth algorithm introduced above. The independence of the edges added naturally implies that given $\mathcal{F}_{\tau-1}$, we have,

$$X_\tau = X_{\tau-1} + \text{Bin}(N - X_{\tau-1}, p_\tau),$$

where p_τ is the conditional probability that an interval is activated by the edge exposure operation in the Interval-Growth algorithm. Given $\mathcal{F}_{\tau-1}$ we can lower bound p_τ as follows.

$$p_\tau \geq \mathbb{P} \left[\text{Bin} \left(\frac{1}{2}L, \mathbb{P} \left[\text{Bin} \left(X_{\tau-1}n^{3/4}a_n, \frac{c}{n} \right) \geq 2 \right] \right) \geq 1 \right].$$

Set $\delta_n \rightarrow 0$ as $n \rightarrow \infty$. On the event $X_{\tau-1} > \varepsilon N$ for some $\varepsilon > 0$, we automatically have $Cn^{3/4+1/16}(\log n)^{1/4}$ infected nodes, and we are already done. Thus we have, on the event $\{X_{\tau-1} \leq N\delta_n\}$

$$\mathbb{E} [X_\tau - X_{\tau-1}] \geq \frac{1}{4} X_{\tau-1}^4 (a_n c)^4.$$

Using Bernstein's inequality, we have, for some universal constant $c_0 > 0$ with probability at least $1 - 2\exp(-c_0 a_n^4)$

$$X_\tau \geq X_{\tau-1}^4 \left(\frac{ca_n}{2} \right)^4.$$

Let us choose $\tau_n = \frac{\log \log n + t_n}{\log 4}$ for some sequence $t_n = t_n(C) = o(\log \log n)$. Then using union bound, the probability that we do not have the desired growth in the number of infected intervals in at least one of the rounds may be upper bounded by $\tau_n \exp(-c_0 a_n^4)$. We note that if we choose $a_n = \log \log n$, the probability of this bad event is $o(1)$.

Moreover, on the good event, we have, $X_{\tau_n} \geq (\frac{ca_n}{2})^{4\tau}$. We choose t_n appropriately such that $X_{\tau_n} \geq Cn^{1/16}(\log n)^{1/4}$. Finally, note that in $\Theta(\log \log n)$ rounds, we grow to length $n^{3/4}a_n \log \log n$ on the first interval, which is $o(L)$, thus indicating that the growth in infected vertices is sustained throughout the first τ rounds. This establishes the desired lower bound on the number of activated intervals in the first τ rounds. \square

Finally, we prove Lemma 1.5.

Proof of Lemma 1.5. Fix any node x in the graph, and consider the interval \mathcal{L}_x along the \mathcal{C}_2 cycle with center at x and of length $n^{3/4}$. If this interval contains a pair of adjacent infected vertices at time T_n , x will be infected by time $T_n + n^{3/4}$ due to complex contagion along the cycle. Thus without loss of generality, consider x such that \mathcal{L}_x does not contain two adjacent infected vertices at time T_n . Let A_x denote the event that \mathcal{L}_x does not contain two adjacent infected vertices at time $T_n + 1$. To establish that for any fixed x , A_x^C has very small probability, note that \mathcal{L}_x contains $\frac{1}{2}n^{3/4}$ disjoint adjacent pairs of vertices. Denoting the number of infected vertices at T_n as I_{T_n} , we observe that the probability that a pair of adjacent vertices are infected by time $T_n + 1$ if both these vertices have at least two neighbors in the set of infected vertices. This event happens with probability at least $\mathbb{P}[\text{Bin}(I_{T_n}, \frac{c}{n}) \geq 2]^2$. The probability of the complement is thus at most $(1 - \mathbb{P}[\text{Bin}(I_{T_n}, \frac{c}{n}) \geq 2]^2)$. Using independence of the adjacent pairs in \mathcal{L}_x , we have,

$$\mathbb{P}(A_x^C) \leq \left(1 - \mathbb{P}\left[\text{Bin}\left(Cn^{3/4+1/16}(\log n)^{1/4}, \frac{c}{n}\right) \geq 2\right]^2\right)^{\frac{1}{2}n^{3/4}} = o\left(\frac{1}{n}\right),$$

for $C > 1$ satisfies $Cc > 2$. Finally, a union bound over the vertices x with no adjacent infected pair in \mathcal{L}_x immediately implies that with high probability, every vertex has an infected adjacent pair within distance $n^{3/4}$ by time $T_n + 1$. Thus we can guarantee that all vertices will be infected by time $T_n + n^{3/4} + 1$, establishing the desired result. \square

C. Simulation results for spread time versus network size. The lower and upper bounds in Theorem 1 are $\Omega(n^{3/4})$ and $O^*(n^{3/4})$, respectively. To investigate the asymptotic spreading time numerically, we have plotted the normalized spreading times versus the network size in Fig. S1.

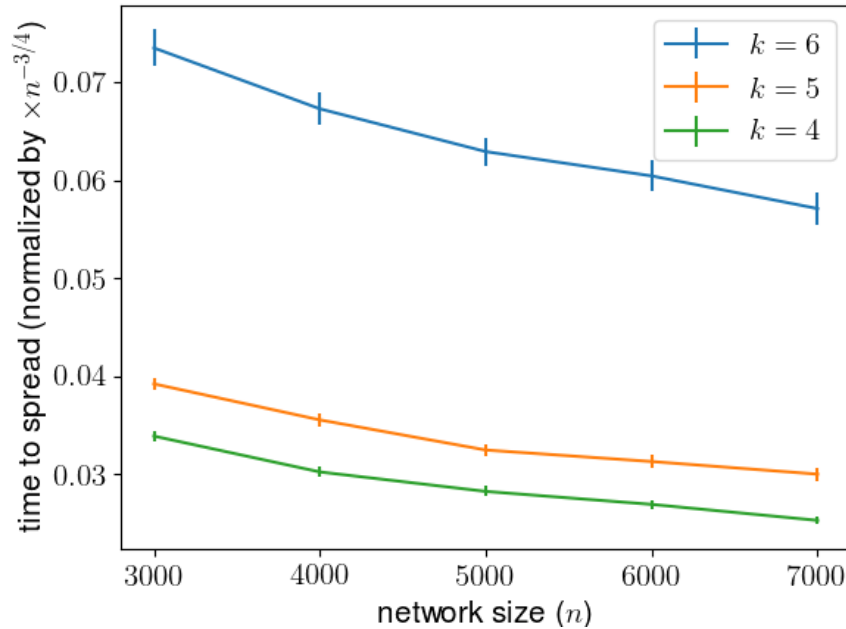


Fig. S1. Spread of Complex Contagion over cycle-power- k union random graphs with the overall expected degree of the nodes fixed at $D = 13$; $\mathcal{C}_k \cup \mathcal{G}_{n,p_n}$, $p_n = (13 - 2k)/n$. Each point is the average of 100 random samples and the error bars show the 95% normal confidence intervals around the means.

2. Complex contagion on \mathcal{C}_1 union random graph with simple adoptions along \mathcal{C}_1 (Theorem 2)

In this section, we consider a model where in addition to complex contagion we have simple contagions along the \mathcal{C}_1 edges, i.e. contagion can spread with probability q_n along \mathcal{C}_1 . In this model, we compare the diffusion speed between $\mathcal{C}_1 \cup \mathcal{G}_{n,2/n}$ and \mathcal{C}_2 . We conclude that for large enough q_n , the contagion spreads faster in $\mathcal{C}_1 \cup \mathcal{G}_{n,2/n}$. Hence, when there is a high enough (but vanishing with increasing n) probability of simple adoptions along the cycle-edges the rewiring of even the \mathcal{C}_2 edges will speed up the spread of complex contagions.

A. Lower-bound on the speed of contagion with simple adoptions. Throughout the subsequent discussion, we denote by I_t the number of infected nodes by time t .

Theorem 2.1 (Upper-bounding the number of infected nodes until $t = o(\sqrt{n}/q_n)$). *Fix $t = o(\sqrt{n}/q_n)$. Then with high probability as $n \rightarrow \infty$, $I_t = o(\sqrt{n})$.*

Proof of Theorem 2.1. Let \mathcal{B}_t be the largest interval on \mathcal{C}_1 containing the initial seed nodes and the neighboring nodes infected by simple contagion along the cycle in time t . Denoting the size of this set as B_t , note that B_t is increasing in t , $B_0 = 2$ and $B_t \rightarrow n$ with probability one as $t \rightarrow \infty$. To complete the proof, we will use the following lemmas.

Lemma 2.2 (Duration of the Initial Simple Contagion Phase). *For $tq_n = o(\sqrt{n})$, $\mathcal{B}_t = o(\sqrt{n})$.*

Lemma 2.3 (Initial Simple Contagion Phase). *Fix $tq_n = o(\sqrt{n})$. With high probability as $n \rightarrow \infty$, none of the nodes outside \mathcal{B}_t are infected.*

The proof of Theorem 2.1 is complete given these lemmas. We prove these assertions in the rest of this section. \square

First we turn to the proof of Lemma 2.2. We will utilize the following lower tail bound on negative binomial random variables.

Lemma 2.4 (Lower Tail Bounds for Geometric Variables). *Let $\mathbf{g}_i, i = 1, \dots, n$ be a sequence of i.i.d. geometric variables with mean $1/\hat{q}_n$, $\hat{x} = \hat{q}_n t$ and consider $\mathbf{G}(\hat{x}) := \sum_{i=1}^{\lfloor \hat{x} \rfloor} \mathbf{g}_i$. If $t\hat{q}_n \rightarrow \infty$ as $n \rightarrow \infty$, then $\mathbf{G}(\hat{x}) > t/2$ with high probability.*

Proof of Lemma 2.4. Let Y_1, Y_2, \dots be a sequence of i.i.d. Bernoulli variables with success probability \hat{q}_n . Then $\mathbf{G}(\hat{x})$ has the same (negative binomial) distribution as the smallest j such that exactly $\lfloor \hat{x} \rfloor$ of Y_1, \dots, Y_j are one (see e.g. (1)). In particular, $\mathbf{G}(\hat{x}) < t/2$ if, and only if, $\sum_{i=1}^{\lfloor t/2 \rfloor} Y_i > \hat{x} = \hat{q}_n t$. We can bound the probability of the latter event by a simple application of Markov inequality for the sum of i.i.d. Bernoulli variables. We have,

$$\mathbb{P} \left\{ \sum_{i=1}^{\lfloor t/2 \rfloor} Y_i > \hat{q}_n t \right\} \leq \frac{\mathbb{E} \left\{ \left(\sum_{i=1}^{\lfloor t/2 \rfloor} Y_i \right)^2 \right\}}{\hat{q}_n^2 t^2} = \frac{(t/2)\hat{q}_n}{\hat{q}_n^2 t^2} = \frac{1}{2t\hat{q}_n} = o(1).$$

Hence, $\mathbb{P}\{\mathbf{G}(\hat{x}) \geq t/2\} \rightarrow 1$ as $n \rightarrow \infty$, completing the proof. \square

Armed with Lemma 2.4, we can now establish Lemma 2.2.

Proof of Lemma 2.2. Let $t = o(\sqrt{n}/q_n)$ and consider the spread of simple contagion along the \mathcal{C}_1 edges up to time t . Starting from two adjacent seeds, the time for the simple contagion to spread to either neighboring node is a geometric random variable with success probability q_n and mean $1/q_n$. In particular, the time that it takes until the first of the two neighboring nodes gets infected is the minimum of two i.i.d. geometric mean $1/q_n$ variables, which is another geometric variable with success probability $\hat{q}_n = 1 - (1 - q_n)^2 = (2 + o(1))q_n$. To upper-bound the number of simple infections up to time $t = o(\sqrt{n}/q_n)$ we can consider a sped up infection process whereby whenever the first of the two nodes at either side of the infected interval is infected we force the second one to be infected as well. Denote the infected interval that results from this sped-up simple infection process by $\hat{\mathcal{B}}_t$, and set $\hat{B}_t = |\hat{\mathcal{B}}_t|$. First we show that $\hat{B}_t = o(\sqrt{n})$ for $t = o(\sqrt{n}/q_n)$. To this end, let $\mathbf{g}_i, i = 1, \dots, n$ be a sequence of i.i.d. geometric variables with mean $1/\hat{q}_n$, and $\mathbf{x}^* := \sup\{x : \sum_{i=1}^x \mathbf{g}_i < t/2\}$. Then $\hat{B}_t = 2 + \mathbf{x}^*$. Let $\hat{x} = \hat{q}_n t$ and consider $\mathbf{G}(\hat{x}) := \sum_{i=1}^{\lfloor \hat{x} \rfloor} \mathbf{g}_i$. Lemma 2.4 implies that $\mathbf{G}(\hat{x}) > t/2$ with high probability whenever $t\hat{q}_n \rightarrow \infty$ as $n \rightarrow \infty$. Thus $\hat{B}_t = 2 + \mathbf{x}^* < 2 + \hat{x} = 2 + t\hat{q}_n = o(\sqrt{n})$ with high probability. Finally, we show that with high probability as $n \rightarrow \infty$, $\mathcal{B}_t \subset \hat{\mathcal{B}}_t$. Note that $\mathcal{B}_t \not\subset \hat{\mathcal{B}}_t$ only if there is at least one vertex which is infected by complex contagion up to time t . We note that occurs with probability $o(1)$ by Lemma 2.3. This establishes that $\mathcal{B}_t \subset \hat{\mathcal{B}}_t$ with high probability. Finally, the case $t\hat{q}_n = O(1)$ follows from the monotonicity of B_t . \square

Finally we establish Lemma 2.3.

Proof of Lemma 2.3. Fix $t = o(\sqrt{n}/q_n)$ and note that Lemma 2.2 implies that there exists a sequence $a_n = o(\sqrt{n})$ such that $\mathbb{P}(B_t < a_n) = 1 - o(1)$. Now, conditional on $\{B_t < a_n\}$, note that for contagion to spread to some node outside of \mathcal{B}_t , there has to be at least one node outside of \mathcal{B}_t that has at least two long ties to the nodes inside \mathcal{B}_t . Therefore

$$\begin{aligned} & \mathbb{P}\{\text{Some node outside } \mathcal{B}_t \text{ is infected}\} \\ & \leq \mathbb{P}\{\text{Some nodes outside } \mathcal{B}_t \text{ has two long-tie to the nodes inside } \} \\ & \leq \mathbb{P}\{\text{Bin}(n - B_t, \mathbb{P}[\text{Bin}(B_t, 2/n) \geq 2]) \geq 1\} = O\left((n - B_t) \frac{4B_t^2}{n^2}\right) = o(1). \end{aligned}$$

Hence for $t = o(\sqrt{n}/q_n)$, with high probability all infected nodes belong to \mathcal{B}_t , and $\mathcal{I}_t = \mathcal{B}_t$. This completes the proof. \square

B. Upper-bound on the speed of contagion with simple adoptions. The next result derives an upper bound on the infection time of all nodes in the graph. Some aspects of the proof are similar to that of Theorem 1.3.

Theorem 2.5. *With high probability, the entire graph will be infected in time $3\frac{\sqrt{n}}{q_n}(\log \log n)^2(1 + o(1))$.*

Proof of Theorem 2.5. As in the proof of Theorem 1.3, we devise an algorithm to lower bound the initial growth of the set of infected nodes. Next, we divide the cycle into consecutive intervals of length $L = \sqrt{n}(\log \log n)^3$. Call an interval *active* if it contains an infected node. Initially, declare the interval containing the original seed nodes as an active interval. Starting with the initial seed nodes, after $2\sqrt{n} \log \log n / q_n$ steps the length of the original interval grows to at least $\sqrt{n} \log \log n$ with high probability. In general, with high probability as $n \rightarrow \infty$, over the first $O(\log \log n)$ iterations of this algorithm, after each set of $2\sqrt{n} \log \log n / q_n$ time steps, the length of infected segments in each active interval will grow at least $\sqrt{n} \log \log n$ due to the simple contagion along the cycle. By revealing the edges of $\mathcal{G}_{n,2/n}$ that are incident to the newly infected nodes at the end of each $2\sqrt{n} \log \log n / q_n$ epoch, we can identify new active intervals that will, in turn, grow and activate other intervals. Formally, we consider the following algorithm to undercount the number of infected nodes. Denote by X_τ the number of active intervals after τ epochs of length $2\sqrt{n} \log \log n / q_n$.

Algorithm: Super-Exponential-Activation

- Initialize:
 - Let $N = \sqrt{n}/(\log \log n)^3$. Divide the cycle into N intervals of length $L_n = \sqrt{n}(\log \log n)^3$ each, and label them by $[N]$; let the initial seed nodes be contained in the interval that is labeled one: $\mathcal{X}_0 = \{1\}$.
- For $\tau \geq 1$, given $\mathcal{X}_{\tau-1}$:
 - Wait an epoch of length $2\sqrt{n} \log \log n / q_n$ and track the growth of infected nodes along the cycle by simple contagion.
 - Add edges independently with probability $2/n$ connecting the new infected nodes to the healthy nodes.
- Update the set of active intervals by adding all intervals that have new infected nodes in them. $\mathcal{X}_\tau \leftarrow \mathcal{X}_{\tau-1}$.

The first lemma derives a lower bound on the number of active intervals after $O(\log \log n)$ steps.

Lemma 2.6 (Initial Growth of the intervals). *For any $C > 0$, there exists a sequence $t_n := t_n(C) = o(\log \log n)$ such that for*

$$\tau_n = \frac{1}{\log 2} \left(\log \log n + t_n \right),$$

with high probability as $n \rightarrow \infty$, $X_{\tau_n} \geq Cn^{1/4}(\log n)^{1/2}$.

Finally, the next result states that with high probability, the contagion process spreads to the whole graph in time $(\tau_n + 4)\sqrt{n}/q_n$.

Lemma 2.7 (End Regime). *Let T_n be the first time that simple contagion infects at least $Cn^{3/4}\sqrt{\log n}$ nodes, where $C > 1$ is a universal constant. Then with high probability, all nodes are infected by time $T_n + 1 + 2\sqrt{n}/q_n$.*

The proof follows upon combining Lemma 2.6 and Lemma 2.7, and noting that $1/\log 2 < 1.5$. \square

We turn to the proof of Lemma 2.6 and Lemma 2.7. We first establish that for the first $O(\log \log n)$ rounds, at least $\sqrt{n} \log \log n$ new nodes are infected over each $2\sqrt{n} \log \log n / q_n$ epoch. To this end, we require the following lemma.

Lemma 2.8. *Fix $\tau_n = \frac{1}{\log 2} \log \log n (1 + o(1))$. With high probability as $n \rightarrow \infty$, every activated interval gains at least $\sqrt{n} \log \log n$ new infected nodes over each of the first τ_n epochs of length $2\sqrt{n} \log \log n / q_n$.*

Proof of Lemma 2.8. We begin with the observation that the waiting time for an activated interval to gain at least $\sqrt{n} \log \log n$ new vertices via simple contagion is a sum of $\sqrt{n} \log \log n$ i.i.d. Geometric random variables, each with mean $\frac{1}{q_n}$. Let $\{g_1, g_2, \dots\}$ be a sequence of i.i.d. Geometric random variables with mean $1/q_n$. Thus during an epoch of length $2\sqrt{n} \log \log n / q_n$, an activated interval fails to gain at least $\sqrt{n} \log \log n$ new infected nodes via simple contagion along the circle if $\sum_{i=1}^{\sqrt{n} \log \log n} g_i > 2\sqrt{n} \log \log n / q_n$. Standard upper tail bounds on sums of geometric random variables (1, Theorem 1.14) directly implies that

$$\mathbb{P}\left[\sum_{i=1}^{\sqrt{n} \log \log n} g_i > 2\frac{\sqrt{n} \log \log n}{q_n}\right] \leq \exp\left(-\frac{\sqrt{n} \log \log n}{4}\right).$$

Note that at each epoch, there are at most \sqrt{n} active intervals. Thus a direct union bound argument over $O(\log \log n)$ rounds of the algorithm establishes that with high probability, each activated interval gains the desired number of infected vertices in at each epoch. It is implicit in the calculation above that the infection of new vertices is sustained as long as an active interval is not exhausted. To this end, note that over a time epoch of length $2\sqrt{n} \log \log n / q_n$, an active interval gains at least $M\sqrt{n} \log \log n$ new infected vertices, for some $M > 1$ is at most

$$\mathbb{P}\left[\sum_{i=1}^{M\sqrt{n} \log \log n} g_i < 2\frac{\sqrt{n} \log \log n}{q_n}\right] \leq \exp\left(-\frac{1}{2} \log\left(\frac{1}{M}\right) \sqrt{n} \log \log n\right),$$

where the last inequality follows using (2, Theorem 3.1). Thus for $M > 1$ sufficiently large, we can guarantee that at each epoch, an active interval gains at most $M\sqrt{n} \log \log n$ many new nodes by simple infection, and thus no active interval is exhausted in the first τ_n rounds with high probability. This completes the proof. \square

Given Lemma 2.8, we can now prove Lemma 2.6.

Proof of Lemma 2.6. Let us denote the natural filtration associated with this growth process as $\{\mathcal{F}_\tau : \tau \geq 1\}$. Note that at the end of $\tau - 1$ steps, we have $X_{\tau-1}$ infected intervals, and thus $N - X_{\tau-1}$ non-active intervals. Each non-active interval is activated if at least one node has two infected neighbors in the Super-Exponential-Activation algorithm described above. The independence of the edges added naturally implies that given $\mathcal{F}_{\tau-1}$, we have,

$$X_\tau = X_{\tau-1} + \text{Bin}(N - X_{\tau-1}, p_\tau),$$

where p_τ is the conditional probability that an interval is activated by the edge exposure operation in the Super-Exponential-Growth algorithm. Let \mathcal{E} denote the good event that each active interval has gained at least $\sqrt{n} \log \log n$ new infected vertices during each epoch of length $\sqrt{n} \log \log n / q_n$ up to the τ^{th} round. Observe that Lemma 2.8 implies that $\mathbb{P}(\mathcal{E}) = 1 - o(1)$. Now, we have, given $\mathcal{F}_{\tau-1}$ we can lower bound p_τ on the event \mathcal{E} as follows.

$$p_\tau \geq \mathbb{P}\left[\text{Bin}\left(L, \mathbb{P}\left[\text{Bin}\left(X_{\tau-1}\sqrt{n} \log \log n, \frac{2}{n}\right) \geq 2\right]\right) \geq 1\right].$$

On the event $X_{\tau-1} > \varepsilon N$ for some $\varepsilon > 0$, we automatically have $Cn^{3/4}\sqrt{\log n}$ infected nodes, and we are already done. Thus we set $\delta_n \rightarrow 0$ as $n \rightarrow \infty$, and note that on the event $\{X_{\tau-1} \leq N\delta_n\} \cap \mathcal{E}$

$$\mathbb{E}[X_\tau - X_{\tau-1}] \geq X_{\tau-1}^2 (\log \log n)^2.$$

Using Bernstein's inequality, we have, for some universal constant $c_0 > 0$ with probability at least $1 - 2\exp(-c_0(\log \log n)^2)$

$$X_\tau \geq X_{\tau-1}^2 \left(\frac{\log \log n}{2}\right)^2.$$

Let us choose $\tau_n = \frac{\log \log n + t_n}{\log 2}$ for some sequence $t_n = t_n(C) = o(\log \log n)$. Then using union bound, the probability that we do not have the desired growth in the number of infected intervals in at least one of the rounds may be upper bounded by $\tau_n \exp(-c_0(\log \log n)^2)$. We note that the probability of this bad event is $o(1)$. Moreover, on the good event, we have, $X_{\tau_n} \geq (\frac{\log \log n}{2})^{2^{\tau_n}}$. We choose t_n appropriately such that $X_{\tau_n} \geq Cn^{1/4}\sqrt{\log n}$. This establishes the desired lower bound on the number of infected nodes in the first τ rounds. \square

Finally we establish Lemma 2.7.

Proof of Lemma 2.7. For a node x , let \mathcal{L}_x denote the interval of length \sqrt{n} on the cycle centered at x . We will show that with high probability, for each x , \mathcal{L}_x contains at least one infected node by time $T_n + 1$. This implies that with high probability, all vertices will be infected by time $T_n + 1 + 2\sqrt{n}/q_n$ due to simple contagion along the cycle. This last assertion follows using upper tail concentration for a sum of geometric random variables and union bound, exactly as described in the proof of Lemma 2.8. Thus we will omit this step in the subsequent argument.

By time T_n , we have at least $Cn^{3/4}\sqrt{\log n}$ infected nodes. For any fixed x , \mathcal{L}_x has \sqrt{n} vertices, the probability that each such vertex has less than two infected neighbors is at most $\mathbb{P}\left[\text{Bin}(Cn^{1/4}\sqrt{\log n}, \frac{2}{n}) < 2\right]$. Using independence of the edges in $\mathcal{G}_{n,2/n}$, the probability that none of the vertices in \mathcal{L}_x is infected by time $T_n + 1$ is at most $(\mathbb{P}\left[\text{Bin}(Cn^{1/4}\sqrt{\log n}, \frac{2}{n}) < 2\right])^{\sqrt{n}}$. Let A_x denote the event that none of the vertices in \mathcal{L}_x are infected by time $T_n + 1$. The analysis above and direct computation immediately implies

$$\mathbb{P}(A_x) \leq n^{-C}.$$

Finally, a union bound over all nodes on the cycle completes the proof, since $C > 1$. \square

C. Simple adoption probabilities under logit and probit Activation functions. In Figure 4B of the main text we present the simulation results for the spreading time of complex contagion over \mathcal{C}_1 union $\mathcal{G}_{n,2/n}$ for various probabilities of simple adoptions q . Our theoretical results in Theorem 2 suggests that having $q = \omega(1/\sqrt{n})$ is enough to ensure a faster spread in $\mathcal{C}_1 \cup \mathcal{G}_{n,1/n}$ compared to \mathcal{C}_2 . Here we derive the corresponding conditions on the parameters of the logit and probit functions to ensure that $q = \omega(1/\sqrt{n})$ under these classes of activation functions. Consider a probit activation function such that the probability of adoptions when the number of infected neighbors is x is given by:

$$\Phi_{\theta, \sigma_n}(x) = \int_{-\infty}^{\frac{x-\theta}{\sigma_n}} \frac{1}{\sqrt{2\pi}} e^{-t^2/2} dt$$

We are interested in the asymptotic regime $\sigma_n \rightarrow 0$ as $n \rightarrow \infty$. We choose $\theta = 1.5$ to ensure a high probability of adoption with two infected neighbors and a low (but non-zero) adoption probability with only one infected neighbor. There is no adoption when there are no infections in the agent's neighborhood. The probability of adoptions below threshold is given by:

$$\hat{q}_n = \Phi_{1.5, \sigma_n}(1) = \int_{-\infty}^{-\frac{1}{2\sigma_n}} \frac{1}{\sqrt{2\pi}} e^{-t^2/2} dt = \int_{\frac{1}{2\sigma_n}}^{+\infty} \frac{1}{\sqrt{2\pi}} e^{-t^2/2} dt$$

Using the Gaussian tail bounds for $x > 0$,

$$\frac{1}{\sqrt{2\pi}} \frac{x}{x^2 + 1} e^{-x^2/2} \leq \int_x^\infty \frac{1}{\sqrt{2\pi}} e^{-t^2/2} dt \leq \int_x^\infty \frac{t}{x} \frac{1}{\sqrt{2\pi}} e^{-t^2/2} dt = \frac{e^{-x^2/2}}{x\sqrt{2\pi}},$$

we get

$$\frac{e^{-1/8\sigma_n^2}}{\sqrt{2\pi}} \left(\frac{2\sigma_n}{1 + 4\sigma_n^2} \right) \leq \hat{q}_n \leq 2\sigma_n \frac{e^{-1/8\sigma_n^2}}{\sqrt{2\pi}},$$

Hence,

$$\hat{q}_n = \Theta\left(2\sigma_n e^{-1/8\sigma_n^2}\right),$$

In particular, taking $\sigma_n = 1/\sqrt{8 \log n^\alpha}$ yields that

$$\hat{q}_n = \Theta\left(\frac{1}{\sqrt{2 \log n^\alpha}} n^{-\alpha}\right),$$

Hence, $\hat{q}_n = o(n^{-1/2})$ for $\alpha \geq 1/2$ and $\hat{q}_n = \omega(n^{-1/2})$ for $\alpha < 1/2$.

We can repeat the same calculations when the activation functions are specified by a logistic function:

$$\Psi_{\theta, \sigma_n}(x) = \frac{1}{1 + e^{(1/\sigma_n)(\theta - x)}}.$$

The probability of adoptions below threshold for logistic activation functions is given by:

$$\tilde{q}_n = \Psi_{1.5, \sigma_n}(1) = \frac{1}{1 + e^{(1/2\sigma_n)}} = \Theta(e^{-1/2\sigma_n}).$$

for $\sigma_n \rightarrow 0$ as $n \rightarrow \infty$. Choosing $\sigma_n = \frac{1}{2 \log(n^\alpha)}$ yields $\tilde{q}_n = \Theta(n^\alpha)$: $\tilde{q}_n = o(n^{-1/2})$ for $\alpha > 1/2$ and $\tilde{q}_n = \omega(n^{-1/2})$ for $\alpha < 1/2$.

Note that $\Phi_{\theta, \sigma}(0) > 0$ and $\Psi_{\theta, \sigma}(0) > 0$; hence, the logit and probit activation functions allow for a small probability of "spontaneous" adoptions even when there are no infected neighboring nodes.

3. Complex contagion over \mathcal{C}_2^η with simple adoptions along \mathcal{C}_1 (Theorem 3)

Theorems 1.1 and 1.3 characterize the time needed for all nodes to be infected by 2-complex contagion on $\mathcal{C}_2 \cup \mathcal{G}_{n, 2/n}$. In comparison, pure complex 2-contagion on \mathcal{C}_4 requires $\Theta(n)$ time to infect all vertices, although the average degree is the same in the two cases. One could naturally envision obtaining $\mathcal{C}_2 \cup \mathcal{G}_{n, 2/n}$ by a "re-wiring" of the edges in \mathcal{C}_4 , and thus from a network intervention viewpoint, the result strongly suggests the usefulness of adding long edges to speed up the complex contagion procedure. However, any further rewiring destroys the 2-core necessary for the spread of complex contagion, and thus will actually stall the infection procedure. Theorems 2.1 and 2.5 amend this picture, and conclude that with the additional presence of a small probability of adoption below threshold, the addition of long edges significantly speeds up the infection procedure.

In this section, we adopt a more dynamical viewpoint, and interpolate between \mathcal{C}_2 and $\mathcal{C}_1 \cup \mathcal{G}_{n, 2/n}$. To facilitate the spread of the infection process on the whole graph, we add a small probability q_n of adoption below threshold along \mathcal{C}_1 . Surprisingly, our findings below indicate that initial rewiring slows down the infection process, whereas after a point, provided q_n is large enough, the infection process spreads faster compared to that of complex contagion on \mathcal{C}_2 .

Formally, we consider the following interpolation model. Consider two random graph processes $\{\mathcal{D}_\eta, \eta \geq 0\}$ and $\{\mathcal{G}_\eta, \eta \geq 0\}$ that are coupled through the common index $\eta \geq 0$. For any fixed $\eta > 0$, the graph processes are distributed as follows.

1. Let $\{X_{ij} : 1 \leq i < j \leq n\}$ be i.i.d. Exponential random variables with rate $1/n^2$. Construct \mathcal{G}_η with vertex set $[n]$, and for any $i < j$, we add an edge connecting the two vertices if $\{X_{ij} < \eta\}$. Therefore, the random graph \mathcal{G}_η is Erdős-Rényi with edge probability $\mathbb{P}\{X_{ij} < \eta\} = 1 - e^{-\eta/n^2}$.
2. Associate with every edge i, j in $\mathcal{C}_2 \setminus \mathcal{C}_1$ an independent exponential variable Y_{ij} with mean $2n$. Retain edge i, j in \mathcal{D}_η if $Y_{ij} > \eta$. Thus the probability that the cycle edge i, j is removed is $1 - e^{-\eta/2n}$.

We will study the spread of contagion on the interpolated graph $\mathcal{C}_2^\eta := \mathcal{C}_1 \cup \mathcal{G}_\eta \cup \mathcal{D}_\eta$ in the regime $\eta = o(n)$. Note that for $\eta = o(n)$, the expected degree of a node in \mathcal{C}_2^η is

$$2 + (n-3)(1 - e^{-\eta/n^2}) + 2e^{-\eta/n} = 2 + (n-3) \left(\frac{\eta}{n^2} + o\left(\frac{\eta}{n^2}\right) \right) + 2 \left(1 - \frac{\eta}{2n} + o(\eta/n) \right) = 4 + o(\eta/n).$$

Hence, for $\eta = o(n)$ the expected average degree in \mathcal{C}_2^η remain fixed and equal to four, which is the degree of nodes in \mathcal{C}_2 . In this formulation, η denotes the expected number of edges that are rewired to construct \mathcal{C}_2^η starting from \mathcal{C}_2 .

For the subsequent analysis, we parametrize $\eta = n^\delta$ for subsequent discussion, and study the infection spread over \mathcal{C}_2^η in two regimes.

- (i) For $0 < \delta < 1/2$ we show that the spread slows down with increasing η . In this regime, two long-ties are unlikely to land on the same node, and thus complex contagion along the long ties is blocked. On the other hand, the rewiring creates single edges along the cycle, which slows down the spread of contagion along the cycle. (for a formal statement see Theorem 3.2 below)
- (ii) For $1/2 < \delta < 1$ we show that contagion takes $O^*(n^{3/2}/\eta + \sqrt{n}/q_n)$ time to spread. For η large enough, \sqrt{n}/q_n is the dominant term that fixes the spreading speed. However, for $q_n \gg 1/\sqrt{n}$ we can specify a range of η for which increasing η increases the speed, with complex contagion spreading through the long-ties. In particular, if $q_n = n^{-1/2+\epsilon}$, then for $1/2 < \delta < 1/2 + \epsilon$, contagion spreads faster for larger values of η . (see Theorem 3.5 below)

A. Speed of Contagion for $0 < \delta < 1/2$. We establish a lower bound on the speed of contagion for $\delta \in (0, \frac{1}{2})$ in this section. We need the following preliminary lemmas. For any graph G , let $\deg_{\min}(G)$ denote the minimum degree in G .

Lemma 3.1 (Unlikely occurrence of complex contagions). *For $\eta = o(\sqrt{n})$, $\mathbb{P}(\deg_{\min}(\mathcal{G}_\eta) \geq 2) = o(1)$.*

Proof of Lemma 3.1. Note that for any vertex $i \in [n]$, its degree in the induced subgraph is distributed as $\text{Bin}(n, 1 - \exp^{-\eta/n^2})$. Thus the probability that a fixed vertex has degree at least two is

$$\mathbb{P}(\text{Bin}(n, 1 - \exp(-\eta/n^2)) \geq 2) = O\left(\frac{\eta^2}{n^2}\right).$$

Thus the expected number of vertices with degree at least two in the subgraph induced by \mathcal{G}_η is $O(\eta^2/n) = o(1)$. This concludes the proof. \square

Armed with this lemma, we can now provide a lower bound on the time to contagion in this regime.

Theorem 3.2 (Lower-bound on the spreading time). *With high probability as $n \rightarrow \infty$, the total spreading time is at least $\frac{n}{2} + \frac{\eta}{4q_n}$.*

Proof of Theorem 3.2. Fix $\delta \in (0, \frac{1}{2})$. First, note that the number of edges deleted in $\mathcal{C}_2 \setminus \mathcal{C}_1$ is distributed as $\text{Bin}(n, 1 - \exp(-\frac{\eta}{2n}))$. We denote this number as M_η . Next, observe that Lemma 3.1 implies that with high probability, none of the vertices may be infected by complex contagion, and the infection has to spread along the cycle. To pass each missing edge in $\mathcal{C}_2 \setminus \mathcal{C}_1$, one incurs an independent $\text{Geo}(q_n)$ waiting time. Setting τ as the time for contagion, we have,

$$\mathbb{P}\left(\tau < \frac{n}{2} + \frac{\eta}{4q_n}\right) \leq \mathbb{P}\left(\sum_{i=1}^{M_\eta} \tau_i < \frac{\eta}{4q_n}\right) + o(1),$$

where $\{\tau_i : i \geq 1\}$ are i.i.d. $\text{Geo}(q_n)$ random variables. By direct computation

$$\begin{aligned} \mathbb{E}\left[\sum_{i=1}^{M_\eta} \tau_i\right] &= \mathbb{E}[M_\eta] \mathbb{E}[\tau_i] = \frac{\eta}{2q_n} (1 + o(1)). \\ \text{Var}\left[\sum_{i=1}^{M_\eta} \tau_i\right] &= \frac{1}{q_n^2} \text{Var}(M_\eta) + \frac{1 - q_n}{q_n^2} \mathbb{E}[M_\eta] = O\left(\frac{\eta}{q_n^2}\right). \end{aligned}$$

Finally, using Chebychev's inequality, we have,

$$\mathbb{P}\left(\sum_{i=1}^{M_\eta} \tau_i < \frac{\eta}{4q_n}\right) \leq 4 \frac{\text{Var}\left[\sum_{i=1}^{M_\eta} \tau_i\right]}{\mathbb{E}^2\left[\sum_{i=1}^{M_\eta} \tau_i\right]} = O\left(\frac{1}{\eta}\right) = o(1).$$

This completes the proof. \square

B. Speed of Contagion for $\delta \in (\frac{1}{2}, 1)$. Let us fix $\delta \in (\frac{1}{2}, 1)$. Let us first concentrate on the spread of infection along the cycle via simple or complex contagion. We initialize the process by infecting two adjacent nodes. The infection spreads via complex two contagion until an edge of \mathcal{C}_2 is missing, when it pays a geometric waiting time. Thus to control how many vertices are infected over certain time periods, one needs a good control on the number of missing \mathcal{C}_2 edges in any sub-interval. The following lemma provides this necessary control.

Lemma 3.3. *Consider an interval \mathcal{I} of length L on the cycle. Let $\mathcal{N}(\mathcal{I})$ denote the number of missing \mathcal{C}_2 edges on this segment. For $\lambda \in (0, 1)$*

$$\mathbb{P}\left[|\mathcal{N}(\mathcal{I}) - \mathbb{E}[\mathcal{N}(\mathcal{I})]| > \lambda \mathbb{E}[\mathcal{N}(\mathcal{I})]\right] \leq 2 \exp\left(-\frac{\lambda^2}{3} \mathbb{E}[\mathcal{N}(\mathcal{I})]\right).$$

Proof of Lemma 3.3. We observe that for any fixed interval \mathcal{I} of length L , the number of missing cycle edges $\mathcal{N}(\mathcal{I}) \sim \text{Bin}(\frac{L}{2}, 1 - \exp(-\eta/2n))$. The thesis follows by a direct application of Chernoff inequality for Binomial random variable. \square

Given Lemma 3.3, we can turn to deriving a lower bound on the spreading time for the infection on the cycle.

Theorem 3.4 (High probability lower-bound on the spreading time). *Fix $t = o(\sqrt{n}/q_n + n^{3/2-\delta})$. With high probability as $n \rightarrow \infty$, the number of infected vertices is $o(n^{3/2-\delta})$.*

Proof of Theorem 3.4. Fix $t = o(\sqrt{n}/q_n + n^{3/2-\delta})$. For any $\varepsilon > 0$, consider an interval of length $L = \varepsilon n^{3/2-\delta}$ centered at the seed nodes. Denote this interval as \mathcal{I} and let $\mathcal{N}(\mathcal{I})$ denote the number of missing cycle edges in this interval. We observe that $\mathcal{N}(\mathcal{I}) \sim \text{Bin}(\frac{L}{2}, 1 - \exp(-\eta/2n))$ and thus $\mathbb{E}[\mathcal{N}(\mathcal{I})] = \frac{L}{2} \frac{\eta}{2n} (1 + o(1)) = \varepsilon \sqrt{n}/4 (1 + o(1))$. Thus we have, by Lemma 3.3

$$\mathbb{P}\left[\mathcal{N}(\mathcal{I}) > \frac{1}{2} \mathbb{E}[\mathcal{N}(\mathcal{I})]\right] \geq 1 - 2 \exp\left(-\frac{\varepsilon}{48} \sqrt{n}\right).$$

Note that the waiting time for the simple contagion along the cycle edges to cover the interval \mathcal{I} is distributed as $\sum_{i=1}^{\mathcal{N}(\mathcal{I})} g_i$, where $\{g_i : i \geq 1\}$ are iid geometric random variables with mean $1/q_n$. For $\delta > 0$ small enough, using (2, Theorem 3.1), we have,

$$\mathbb{P}\left[\sum_{i=1}^{\mathcal{N}(\mathcal{I})} g_i < \delta \frac{\mathcal{N}(\mathcal{I})}{q_n} \mid \mathcal{N}(\mathcal{I})\right] \leq \exp\left(-\frac{\delta}{2} \mathcal{N}(\mathcal{I})\right).$$

Thus with high probability as $n \rightarrow \infty$, for simple contagion along the cycle to cover \mathcal{I} , the waiting time to cross the single edges is at least $\frac{\varepsilon \delta \sqrt{n}}{8 q_n}$. Further, Lemma 3.3 implies that the number of missing \mathcal{C}_2 edges is $O(\sqrt{n} \log n)$ with high probability. As a consequence, $n^{3/2-\delta} - \mathcal{N}(\mathcal{I}) = n^{3/2-\delta} (1 - o(1))$ with high probability. For complex contagion to spread along the cycle, the spreading time required is $\Theta(n^{3/2-\delta})$ with high probability. Thus with high probability as $n \rightarrow \infty$, contagion along the cycle covers only a subset of the vertices in \mathcal{I} .

Finally, we will prove that with high probability as $n \rightarrow \infty$, no vertex outside \mathcal{I} is infected by complex contagion along the long ties. To this end, note that a vertex is infected if it has at least two edges to the infected nodes. The probability of infection of each node is upper bounded by $\mathbb{P}[\text{Bin}(L, 1 - \exp(-\eta/n^2)) \geq 2]$. Thus the expected number of infected vertices is at most $n \mathbb{P}[\text{Bin}(L, 1 - \exp(-\eta/n^2)) \geq 2] = O(\varepsilon^2)$. The required claim follows using Markov inequality, once we note that $\varepsilon > 0$ is arbitrary. This completes the proof. \square

The next theorem derives an upper bound to the spreading time for the infection in the regime $\frac{1}{2} < \delta < 1$.

Theorem 3.5 (High probability upper-bound on the spreading time). *Fix $\delta \in (\frac{1}{2}, 1)$. Then with high probability as $n \rightarrow \infty$, all nodes are infected by time $3(\sqrt{n}/q_n + n^{3/2}/\eta)(\log \log n)^2(1 + o(1))$.*

Proof of Theorem 3.5. The proof is similar to that of Theorem 2.5 and thus we only sketch the proof, describing in detail the differences in this case. The proof again proceeds in two stages— in the first stage, we lower bound the growth of infected nodes in the original process and establish that $\Theta(n^{5/4-\delta/2} \sqrt{\log n})$ vertices are infected in about $O((n^{3/2-\delta} + \sqrt{n}/q_n) \log \log n)$ steps. An independent argument establishes that all vertices are infected in $O(n^{3/2-\delta} + \sqrt{n}/q_n)$ additional time. Formally, we establish the following results.

Lemma 3.6. For any fixed $\delta \in (\frac{1}{2}, 1)$ and $C > 1$, there exists a sequence $t_n := t_n(C, \delta) = o(\log \log n)$ such that with high probability as $n \rightarrow \infty$, the infection spreads to $Cn^{5/4-\delta/2}\sqrt{\log n}$ nodes in at most $3(n^{3/2-\delta} + \sqrt{n}/q_n) \log \log n(\log \log n + t_n)$ steps.

Lemma 3.7. Let T_n be the first time when the contagion infects $Cn^{5/4-\delta/2}\sqrt{\log n}$ nodes, where $C > 1$ is a universal constant. Then with high probability, all nodes are infected by time $T_n + 2(\frac{\sqrt{n}}{q_n} + n^{3/2-\delta})$.

The proof follows. \square

Proof of Lemma 3.6. As before, we divide the $[n]$ nodes into N equal intervals of length $L = n^{3/2-\delta}(\log \log n)^3$. We call an interval *active* if it contains at least one infected node. At time zero, we call the interval containing the original infected nodes as active. We will undercount the original growth of infected vertices by a more tractable growth process. To this end, we look at the infection process at epochs of size $(n^{3/2-\delta} + \sqrt{n}/q_n) \log \log n$, and index the epochs by $\tau \geq 1$. During each epoch, the active intervals gain new infected nodes due to infection along the cycle edges. At the end of an epoch, we expose the long range random edges. This in turn, leads to new active intervals, and provides a lower bound on the growth of infected nodes in the original process. We denote the natural filtration associated with the undercounting process as \mathcal{F}_τ , and let X_τ denote the number of infected intervals after τ epochs. In each epoch, with high probability, an infected node further infects its neighbor within $2 \log n/q_n$ time. Once we have two neighboring infected vertices, infection spreads along the cycle via simple and complex contagion. Consider the one-sided interval of length $\frac{1}{2}n^{3/2-\delta} \log \log n$ on any active interval. Lemma 3.3 implies that with high probability, the maximum number of missing cycle edges is $\frac{1}{2}\sqrt{n} \log \log n$. The total weight time to cross these missing edges is $\sqrt{n} \log \log n/q_n$. Thus the contagion process along the cycle infects at least $\frac{1}{2}n^{3/2-\delta} \log \log n$ new nodes in each active interval in each epoch. Note that given $\mathcal{F}_{\tau-1}$,

$$X_\tau - X_{\tau-1} = \text{Bin}(N - X_{\tau-1}, p_\tau).$$

where p_τ is the conditional probability of activation of an inactive interval due to the edge-exposure step at this round. We can lower bound this probability as

$$p_\tau \geq \mathbb{P}\left[\text{Bin}\left(L, \mathbb{P}\left[\text{Bin}\left(\frac{X_{\tau-1}}{2}n^{3/2-\delta} \log \log n, 1 - \exp(-\eta/n^2)\right) \geq 2\right]\right) \geq 1\right].$$

Thus conditional on $\mathcal{F}_{\tau-1}$, we have the lower bound

$$\mathbb{E}[X_\tau - X_{\tau-1}] \geq \frac{1}{8}X_{\tau-1}^2(\log \log n)^2$$

Using Bernstein inequality, we can guarantee that this growth is sustained over the first $O(\log \log n)$ epochs, exactly as outlined in the proof of Lemma 2.6. The proof now follows using arguments outlined in the proof of Lemma 2.6. \square

Proof of Lemma 3.7. Fix a node x and let \mathcal{L}_x be the interval of length $L = n^{3/2-\delta}$ centered at x . The probability that any fixed vertex in this interval has at least two infected neighbors is at least $\mathbb{P}[\text{Bin}(Cn^{5/4-\delta/2}\sqrt{\log n}, 1 - \exp(-\eta/n^2)) \geq 2]$. Using independence of the edges, the probability that no vertex in the interval has at least two infected neighbors is at most $(\mathbb{P}[\text{Bin}(Cn^{5/4-\delta/2}\sqrt{\log n}, 1 - \exp(-\eta/n^2)) < 2])^{n^{3/2-\delta}}$. Denoting this event as A_x , we have,

$$\mathbb{P}(A_x) \leq n^{-C}$$

for $C > 1$. By a union bound, with high probability, each node has at least one infected node in the interval of length L surrounding it. Using union bound, each new infected node further infects a neighbor by simple contagion in $2(\log n)/q_n$ additional time. Further, using Lemma 3.3 and a union bound, the maximum number of missing $\mathcal{C}_2 \setminus \mathcal{C}_1$ edges in any interval \mathcal{L}_x is at most \sqrt{n} . Further, an application of (1, Theorem 1.14) and union bound implies that the total passage time across the missing edges in any interval is at most $2\sqrt{n}/q_n$. Finally, complex contagion covers the remaining interval in $n^{3/2-\delta}$ steps. Thus with high probability, the entire graph is infected by time $T_n + 2(\sqrt{n}/q_n + n^{3/2-\delta})$. \square

C. Simulation results allowing for simple adoptions along all edges. Figure S2 is a redone of the simulation results presented in Figure 4C of the main text, allowing for simple contagion probability q along all edges in the network. Both figures reveal the same kind of qualitative behavior in that, rewiring accelerates the spread for large enough values of q . Moreover, comparisons of the two figures reveal interesting consequences of the handicap assumption that we impose on the model in Figure 4C, by allowing simple contagions only along the C_1 edges.

Not only the spread is accelerated for much smaller values of simple adoption probability ($q \geq 0.0129$) in Figure S2 compared to Figure 4C, but also the initial slow down phase is no longer present in Figure S2. To the contrary, the first few rewired edges are the most effective in accelerating the spread: we observe diminishing returns in the acceleration (or deceleration) of contagion with the number of rewired edges in Figure S2.

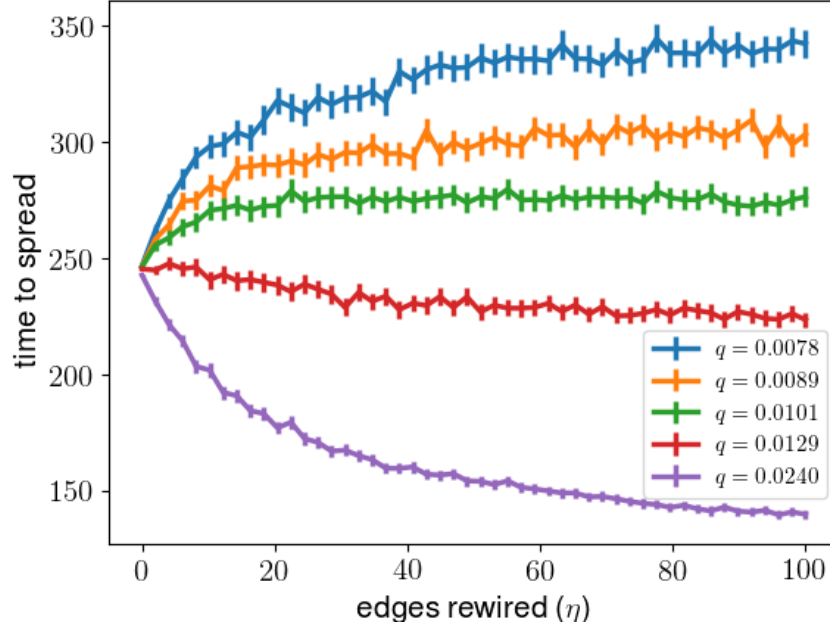


Fig. S2. Spreading time of complex contagion over C_2^η random graphs with $n = 500$, allowing for simple contagion with probability q along all edges (not just C_1). Each point is the average of 1000 random draws and the error bars show the 95% normal confidence intervals around the means.

4. Additional simulations with real network data (robustness studies)

We use three data sets that contain the social networks for 175 rural Chinese farmers being encouraged to sign up for insurance (3), health advice networks collected from 17 rural villages in Uganda (4), and the study of participation in a microfinance program in 77 villages in South India (5). We expand on the results of simulations that we presented in the main text by providing additional statistics and measurements over these networks. Moreover, we provide simulations with variations of the original model to verify the robustness of our claims to changes in the model.

For each village in the three data sets we are interested in how interventions that modify the network structure would affect the spread of contagion. We consider three intervention strategies: (i) random rewiring, (ii) adding new edges uniformly at random, (iii) adding new edges at random with probability proportional to the number of open triads that each new edge would close. Following the same conventions as in Figure 6 of the main text, we use black, orange, blue, and red colors to plot the values corresponding to the original network, as well as the modified networks under rewiring, triad-closing and random edge additions. The intervention sizes are measured in terms of the percent of edges in the original networks. We vary the intervention sizes between 5% and 25%.

In any given network, starting from two randomly chosen seeds (initially infected nodes) we measure the time until 90% of the nodes are infected. Under each intervention and model of contagion that we are considering, we draw 500 random spreading time samples over the original or modified networks and compare the spreading times in terms of their empirical cumulative distribution functions (ECDFs). On a few occasions we combine these samples for all the villages over the entire data set and compare the overall ECDFs for the spreadings times: Figures S4, S5, as well as the second and forth rows in Figure S6 are generated this way. Unless otherwise specified, the intervention size is fixed at 10%: Figure 6 in the main text, as well as Figures S4 and S7, here, follow this convention. When varying the intervention size, we group the samples by their intervention size. The intervention size in each group is fixed at 5, 10, 15, 20 or 25%: Figures S5 and S6 are generated in this manner. In the first and third row of Figure S6 we have overlaid the ECDFs of spreading time for individual villages in the respective data sets (77 villages from the south Indian villages data set (5) in the first row, and 17 villages from the Ugandan villages data set (4) in the third row). In these two cases (the first and third rows of Figure S6) since different village sizes affect the time to total spread, we normalize the spreading times relative to the mean spread time in the original village (with no interventions); moreover, we put the x-axis in logarithmic scale to symmetrize the ratios below and above one.

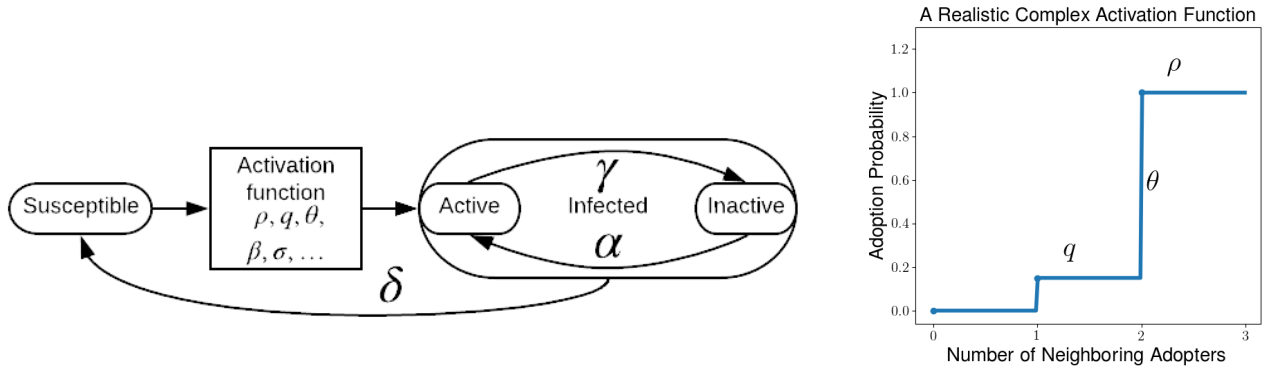


Fig. S3. The model

Figure S3 shows the block diagram of the model that we have implemented for each agent in our simulations. The active and inactive infected states describe a situation where adopter agents may transition into a state where they are not effective in turning their neighboring non-adopters into adopters. We refer to this state as an inactive infected state and allow infected agents to transition back and forth between active and inactive states with probabilities α and γ as depicted in Figure S3. In the basic model that we study in the main text all infected agents are regarded as active; hence, $\alpha = 1$ and $\gamma = 0$. In general, we also allow a probability δ for infected agents to transition back into the susceptible state; however, in our studies we set $\delta = 0$, as motivated by applications where infection connotes product purchase.

The activation function block determines the type of contagion (simple or complex). Different models of contagion are characterized by different parameters. For example, the simple contagion activation functions shown in Figure 1 are parametrized by the independent transmission probabilities (β) along each edge. The probability of infection with x infected neighbors under this simple contagion activation function is given by $1 - (1 - \beta)^x$. On the other hand, the

complex contagion activation function shown in Figure S3 is parametrized by a threshold value θ , adoption probability above threshold ρ , and adoption probability below threshold q . Similarly, logit and probit activation functions studied in Section 2C are characterized by a threshold θ and noise (or “rationality”) level σ . Unless otherwise specified, we compute the spreading time samples under the (0.05, 1) model from Figure S4a ($\rho = 1$, $q = 0.05$, $\alpha = 1$, $\gamma = 0$, $\theta = 2$): the spreading time samples in Figures S6 and S7, here, as well as Figure 6 of the main text are generated under the (0.05, 1) model.

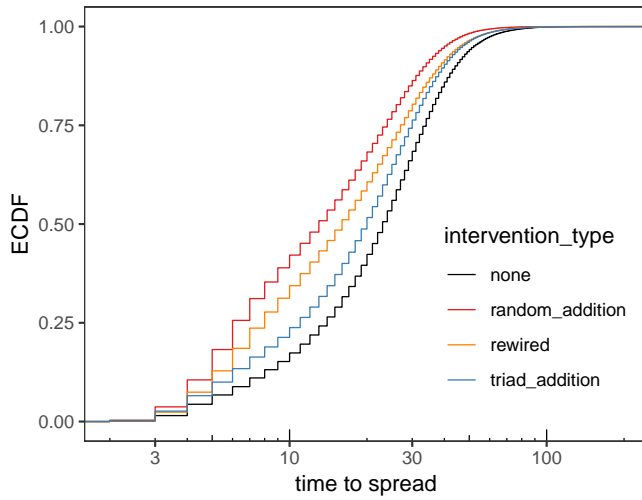
In special cases (Figure S4d, here, and Figure 4C in the main text) we make a distinction between what edges pass simple contagion adoptions (probability q) and what edges do not. Such models are not fully specified by the choice of activation functions and transition probabilities α , γ , and δ , since we need to take into account the type of network edges along which transitions occur. In Figure S4d, we allow the simple contagion probability q only if the edge connecting the adopter and non-adopter agent is existent in the original network. Spreading time samples for this model are collected only under the edge addition interventions (random versus triad-closing). In Figure 4C of the main text we consider the spreading time over \mathcal{C}_2^n random graphs and allow for simple contagion probability q only along the \mathcal{C}_1 cycle edges.

Figure S4 shows the overall ECDFs (combining all samples across all villages with 500 random samples per village) of the spreading times over the Chinese farm villages data set in (3). We present the results for six different models and activation function settings with 10% sized interventions. A more fine-grained version of this data where intervention sizes are varied between 5, 10, 15, 20, and 25% is presented in Figure S5. The two models labeled by (0.05, 1(0.05, 0.5)) and (0.001, 1) in Figures S4c and S4f (see the Figure captions for the corresponding model parameters) are significantly slower. In their ECDFs, we can identify a fast and a slow regime which we attribute to complex and simple contagions, respectively. If the 90% spread is reliant on complex contagion, then the spreading time samples are visibly discrete and the total spread is achieved fast. If, on the other hand, a significant number of nodes are infected through simple contagion (coin flips with probability q), then contagion is slow and spreading time samples cover a wide range, resulting in a smooth section in the ECDF curve.

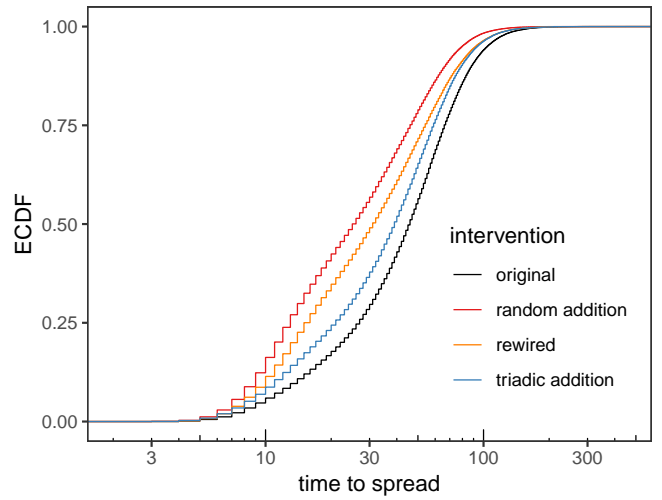
In contrast, the fractional threshold model that is labeled by REL(0.05, 1) in Figure S4e is significantly faster; its ECDF is visibly discrete and does not contain a smooth, slow section. Under this fractional model a node is infected with high probability ($\rho = 1$) if the majority of its neighbors are adopters ($\theta^* = 0.5$); in particular, a leaf node with only one neighbor becomes an adopter as soon as its neighbor adopts. This is in contrast to the absolute threshold model $\theta = 2$ where a leaf node can only be infected through the slow simple contagion (coin flips) with probability q .

In Figure S6 we present the ECDFs for the spreading times over the south Indian (5) and Ugandan (4) villages as well. These figures follow the same conventions as in Figure 6 of the main text, and show the results for different intervention sizes (the intervention size in Figure 6 was fixed at 10%). To further demonstrate the stochastic dominance relation between the spreading times (as random variables) under various interventions, in Figure S7 we present the difference between the ECDFs with 10% interventions for all the villages in the three data sets. The spreading samples in both Figures S6 and S7 are generated under the (0.05, 1) model from Figure S4a ($\rho = 1$, $q = 0.05$, $\alpha = 1$, $\gamma = 0$, $\theta = 2$). If the positive difference persists throughout the entire support of two ECDFs, then we conclude the stochastic dominance relation between their respective random variables.

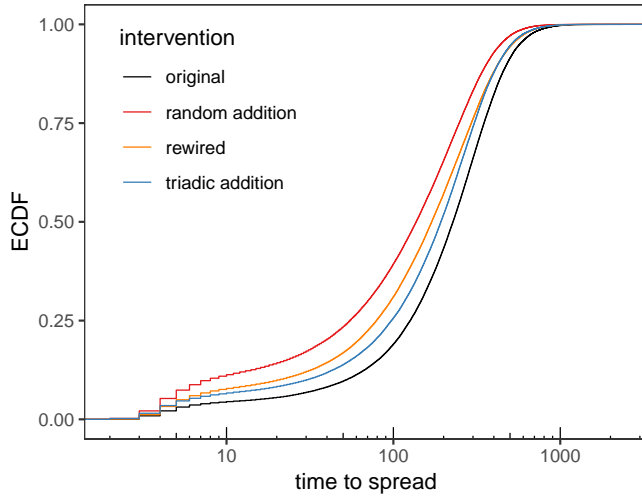
In all these measurements, we observe the same direction (sign) for the effect of interventions on the spreading time: (i) rewiring speeds up the spread of contagion compared to the original networks, (ii) contagion spreads faster in the networks with added edges compared to the original networks, (iii) contagion spreads faster in the network with added random edges compared to the network with added triad-closing edges. The magnitude of differences are larger for larger interventions.



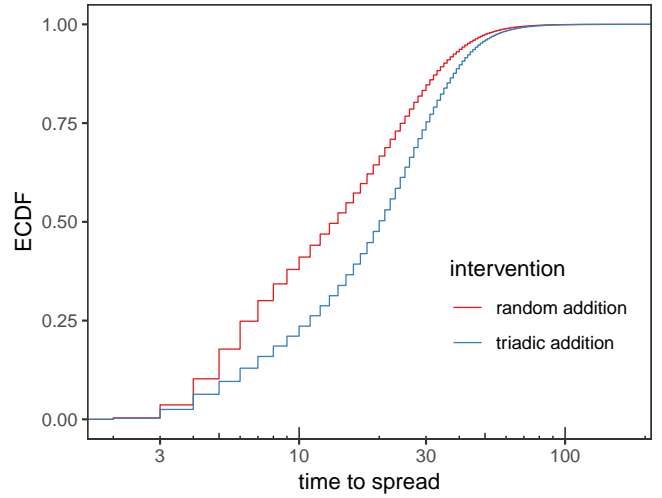
(a) $(0.05, 1) : \rho = 1, q = 0.05, \alpha = 1, \gamma = 0, \theta = 2$



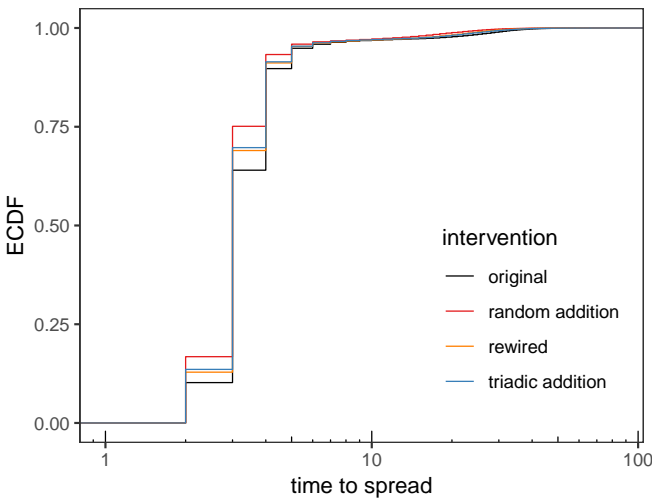
(b) $(0.025, 0.5) : \rho = 0.5, q = 0.025, \alpha = 1, \gamma = 0, \theta = 2$



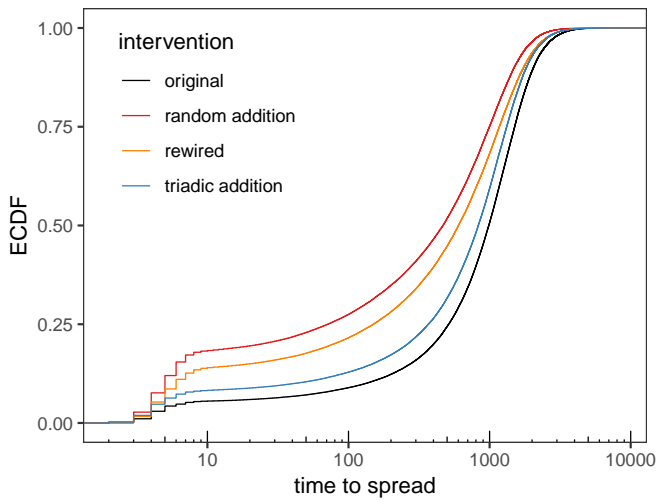
(c) $(0.05, 1(0.05, 0.5)) : \rho = 1, q = 0.05, \alpha = 0.05, \gamma = 0.5, \theta = 2$



(d) $(\text{ORG-}0.05, 1) : \rho = 1, q = 0.05, \alpha = 1, \gamma = 0, \theta = 2$, simple adoptions happen only along the original edges and spreading time samples are collected only under edge addition interventions (triadic vs random)



(e) $\text{REL}(0.05, 1) : \rho = 1, q = 0.05, \alpha = 1, \gamma = 0, \theta^* = 0.5$, complex contagion with fixed common fractional threshold (θ^*)



(f) $(0.001, 1) : \rho = 1, q = 0.001, \alpha = 1, \gamma = 0, \theta = 2$

Fig. S4. The overall ECDF for the spreading times over Chinese farm villages (3) under different contagion models and interventions with fixed size (10%)

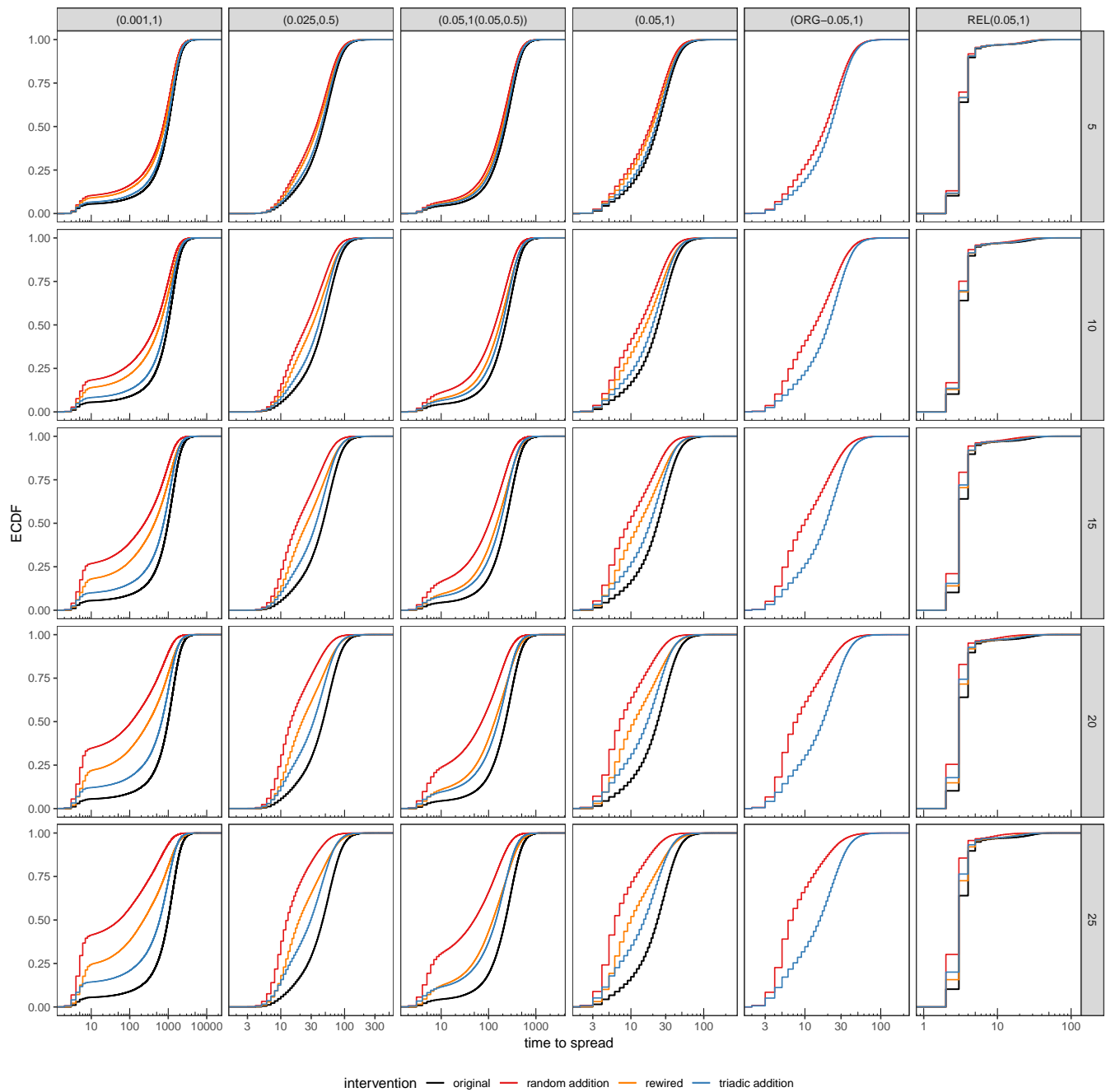


Fig. S5. Overall ECDFs under various interventions grouped by the intervention sizes and contagion models for the Chinese farming villages (3). The model labels at the top are as introduced in the captions of Fig. S4. The intervention sizes are shown on right side.

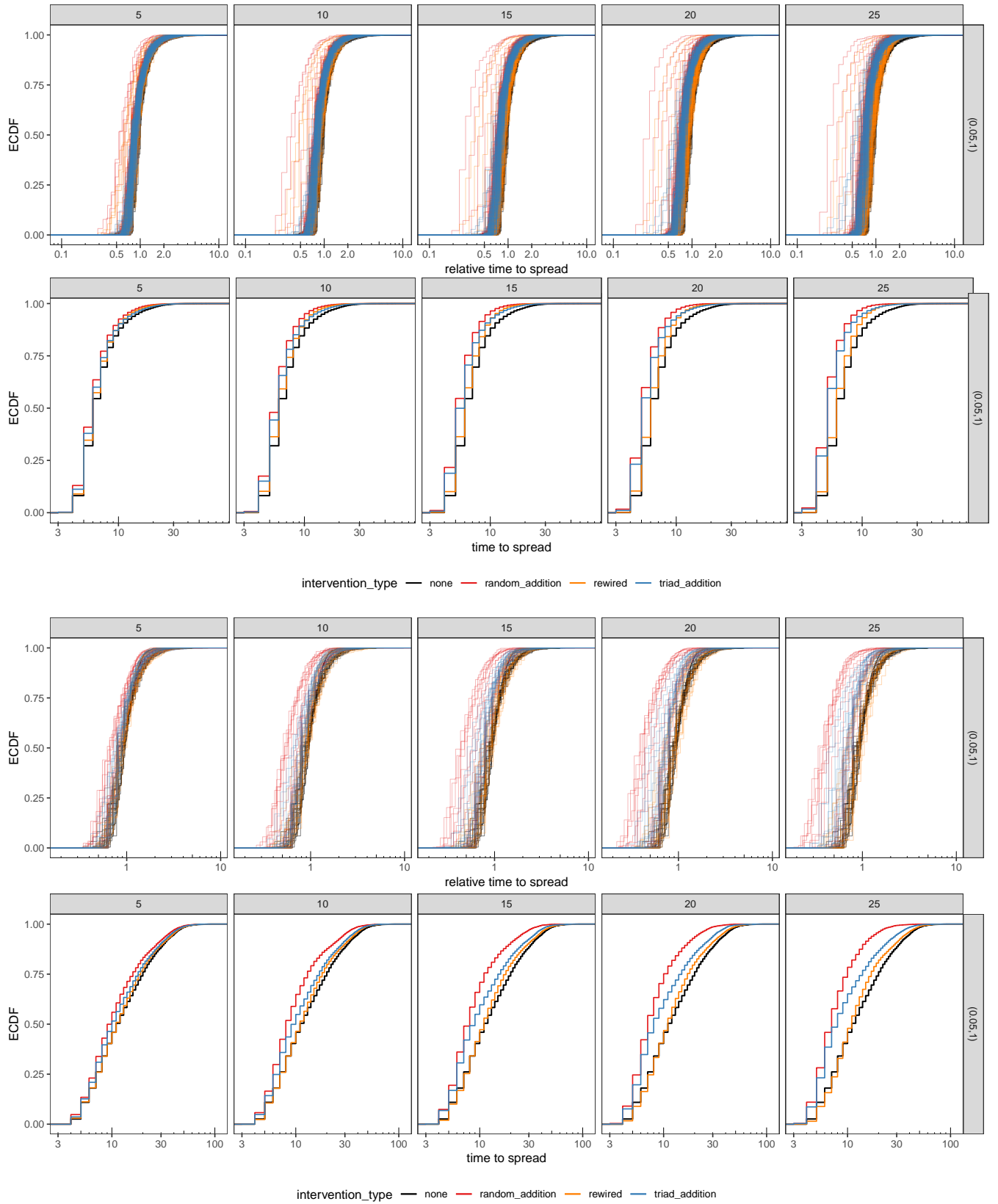


Fig. S6. ECDFs under various interventions grouped by the intervention size for the South Indian (5, top two) and Ugandan (4, bottom two) villages. For each dataset, the top figures show the ECDFs for the individual villages (overlaid) and the bottom figures combine the random samples (spreading times) over the entire dataset. These figures follow the same conventions as Figure 6 of the main text.

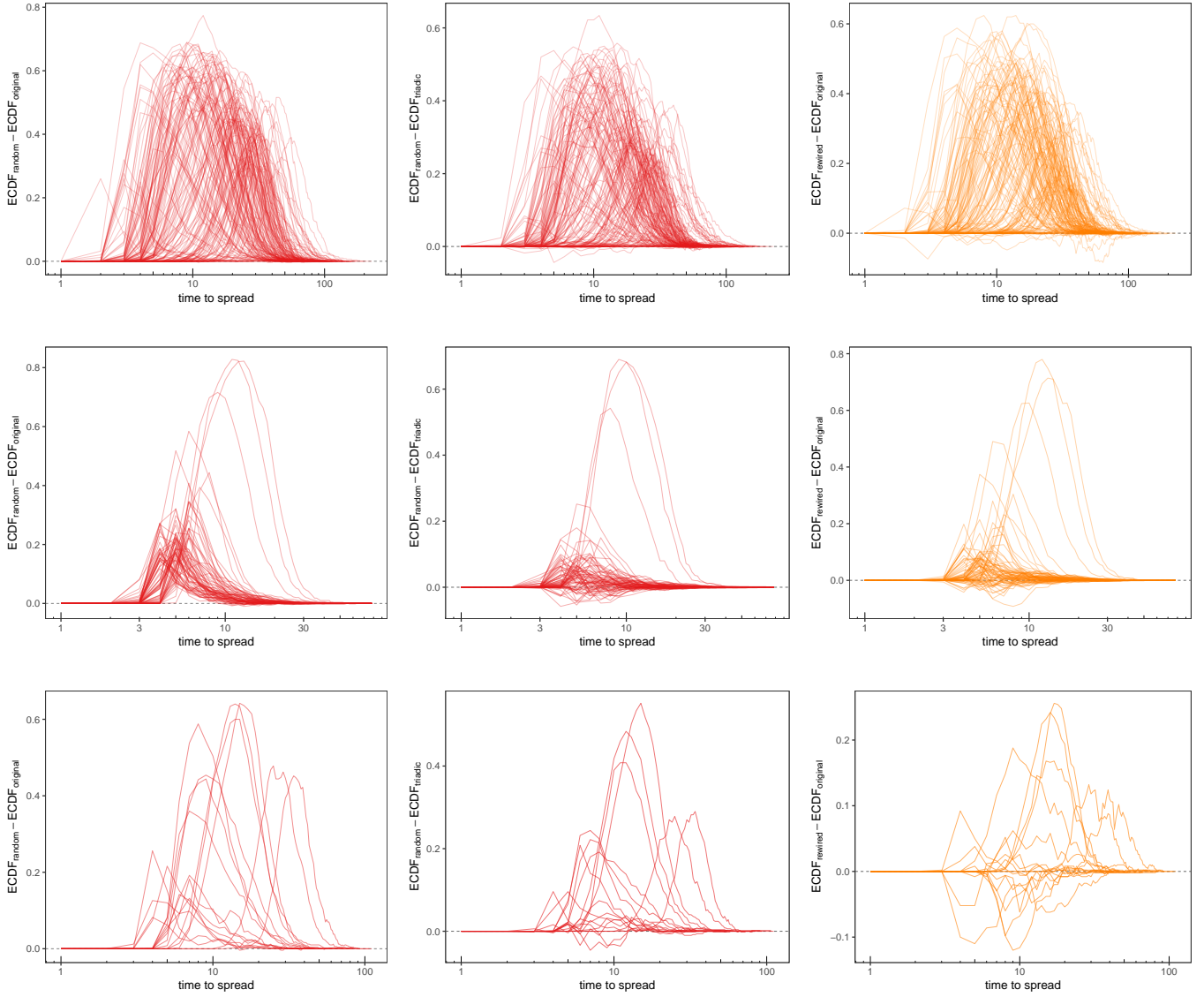


Fig. S7. Difference between spreading time ECDFs in networks with 10% additional random edges and the original ones (leftmost), between the networks with 10% additional random and triad closing edges (middle), and between the 10% rewired and the original networks (rightmost), for the Chinese (3, top), South Indian (5, middle) and Ugandan (4, bottom) villages. The positive differences indicate the stochastic dominance relation between the spread times (as random variables) under one intervention over another. The spreading time samples are computed under the $(0.05, 1)$ model from Figure S4a with $q = 0.05$, $\alpha = 1$, $\gamma = 0$, and $\theta = 2$.

References

1. Doerr B (2011) Analyzing randomized search heuristics: Tools from probability theory in *Theory of Randomized Search Heuristics: Foundations and Recent Developments*. (World Scientific), pp. 1–20.
2. Janson S (2018) Tail bounds for sums of geometric and exponential variables. *Statistics & Probability letters* 135:1–6.
3. Cai J, De Janvry A, Sadoulet E (2015) Social networks and the decision to insure. *American Economic Journal: Applied Economics* 7(2):81–108.
4. Chami GF, Ahnert SE, Kabatereine NB, Tukahebwa EM (2017) Social network fragmentation and community health. *Proceedings of the National Academy of Sciences* 114(36):E7425–E7431.
5. Banerjee A, Chandrasekhar AG, Duflo E, Jackson MO (2013) The diffusion of microfinance. *Science* 341(6144):1236498.